RAL MICE Hall Project

A further investigation of substructure and simplification modelling for the RAL MICE Hall

Prepared by Chris Riley and Klaus Höffer

Introduction

The models of RAL MICE Hall constructed in Opera-3d are very large (in some cases about 19 million finite elements). Nevertheless, some of the geometric items included have required considerable simplification. One of the aims of the project team for MICE is to investigate the possibility of using field values extracted from the overall model as a “source” to a more detailed model of the simplified geometries.

As shown in the report on Validation and Improvement Suggestions for MICE Experimental Hall Modelling, omitting substructure from the model altogether is not valid when the source fields are obtained. However, a simplified model of the substructure can be included. In this report, different options for simplified substructure models are investigated and some indications of probable error associated with the simplification are obtained.

It is not viable to build a real model of the geometry (that has previously been simplified) within the very large model to test this possibility. However, it is possible to build some representative models of typical structures with a simple magnetic source field where both the “real” model and the type of simplifications used within the MICE Hall model can be solved. It is then possible to extract the fields from the simplified structure model and use them as a source to a model that only comprises the detailed substructure being investigated. Comparison with the “real” model will give an indication of the accuracy of using field extraction to model substructures.

Example models

Two example models have been chosen for these purposes. Both of these are areas of concern to the MICE team and, while the real geometry of these structures in the MICE Hall has not been used, they will adequately illustrate the level of error associated with doing substructure models.

Substation model

The first example model is a representation of a substation for a power supply, as shown in figure 1. Two of the side panels of the surrounding steel tank have been removed to view the internal structure in this figure.

The external tank of the substation is a 2 x 2 x 2 metre box made of mild steel (Opera mild average BH curve) plates 0.02 metres thick. The lid of the tank is larger than the tank box and overlaps it by 0.1 metres. Within the tank is a 3-leg transformer yoke (which could be suitable either for a single phase or 3-phase electricity supply) made from a high quality steel (Opera 1010 steel BH curve). The exterior dimensions of the yoke are 1.8 x 1.4 x 0.4 metres and it is placed closer to the floor of the tank and the rear wall. Attached to the front wall of the tank is a separate chamber for housing instruments and controls also made from 0.005 metre thick mild steel. The outside dimensions are 0.9 x 0.4 x 0.13 metres. A small opening representing an opening for a meter or a control panel has been cut into the front wall of the tank (not visible in this view). The centre of the tank is at (0,0,0).

This model is energized by a solenoid coil 2 metres in length and 1.2 metres outside diameter with its centre at (-3,2,-2.5). The field on axis calculated using the Biot-Savart expression is shown in figure 2.

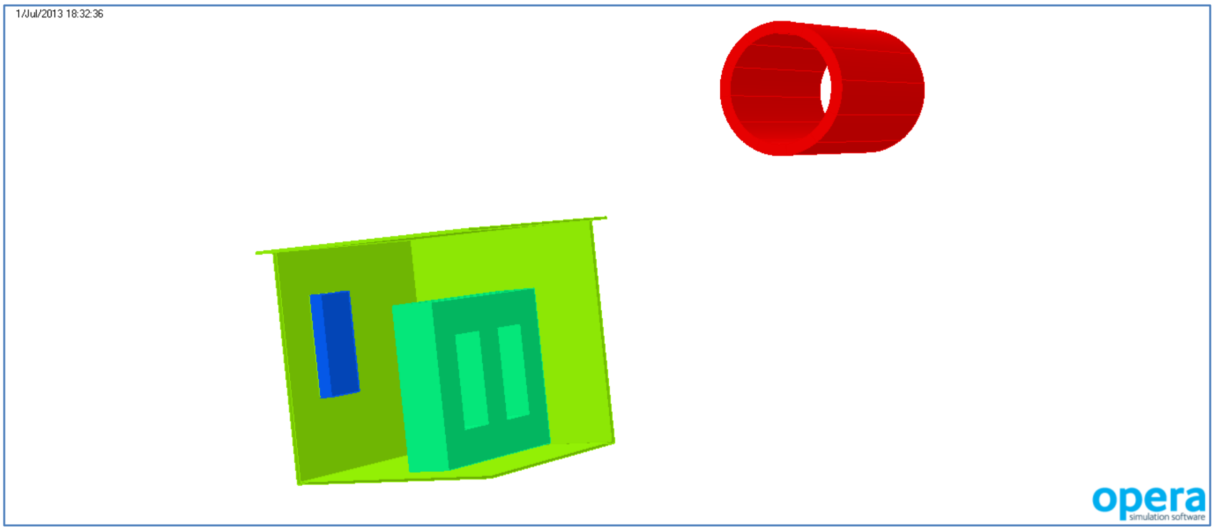

Figure 1: Geometry of substation model

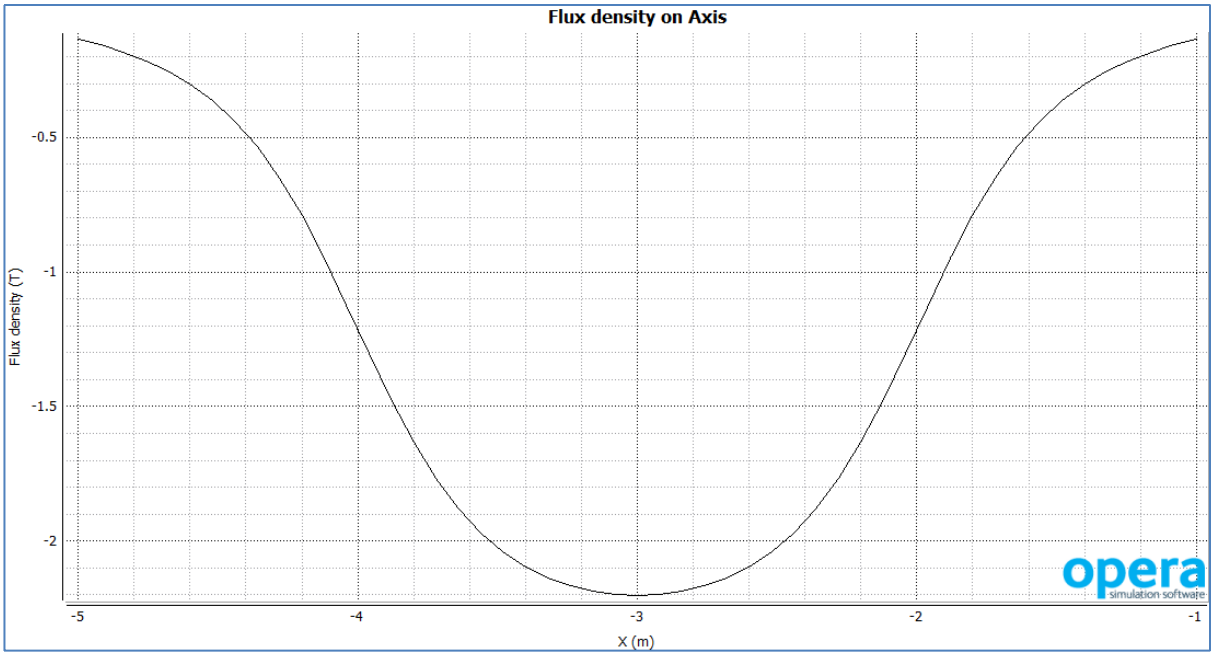

Figure 2: Field on axis

Shielding wall model

The second example represents a typical shielding wall constructed of 4 x 1010 steel plate panels which have been attached to structural I-beams made from mild steel, as shown in figure 3. The panels of the wall are 5 x 1.9 x 0.025 metres and they are attached to the I-beams such that there is 0.1 metre spacing between them, making the overall length of the wall 7.9 metres.

Each I-beam is 0.225 x 0.2 metres overall cross-section and the thickness of the steel is 0.05 metres throughout. Hence, the overlap of the I-beams and the steel panels is also 0.05 metres on each side.
The model is energized by the same solenoid coil as the substation model but it has been moved such that its centre is now at (-3,0,-2.5). The centre of the front face of the wall closest to the solenoid is at (-4,0,0) – although that point is actually in the gap between two of the panels. Consequently, symmetry at Y=0 can be exploited.

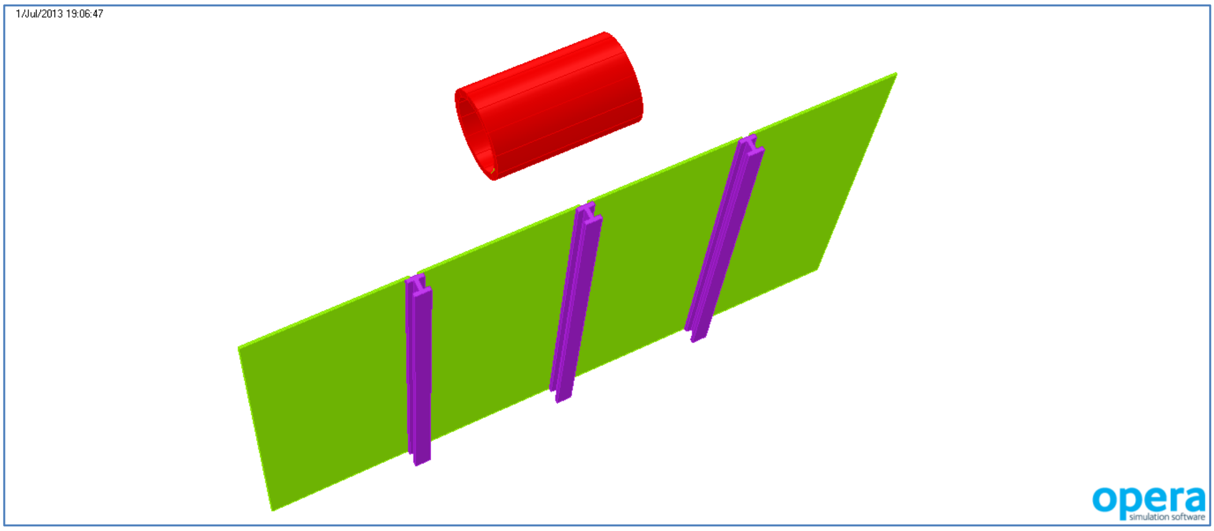

Figure 3: Shielding wall example model

Substation model

Effect of finite element discretization

Figure 4 shows the overall finite element model for the substation model. All AIR material is total potential except the cell immediately surrounding the coil. Some faces of the model have been hidden for clarity.

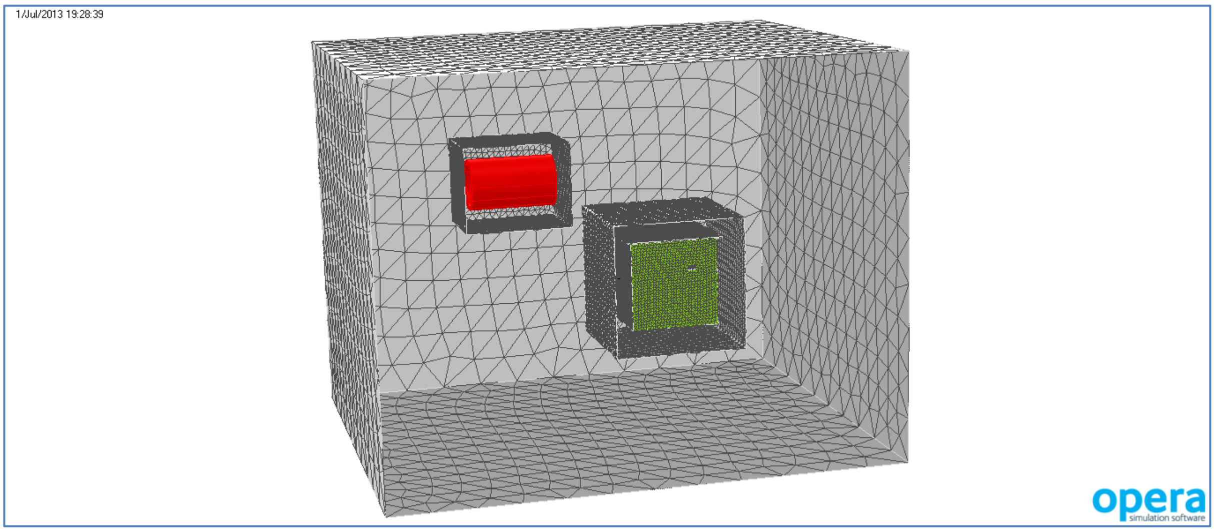

Figure 4: Finite element mesh for "real" substation model

Before determining the effect of simplifications to this model and the use of results from the simplified model as a source to a substructure model, the effect of solving an approximate finite element model should be determined. Two attributes will be important: (1) the size of the finite elements and (2) the truncation of the far-field. The latter of these is particularly important as this has been a necessary constraint on the MICE model and implies images of the model.

A simple test to look at this is to solve the model with all materials set with AIR properties. A perfect finite element model would give results that were identical to the fields from the Biot-Savart expressions. Consequently, the approximations associated with solving using an "imperfect" finite element mesh can be determined.

In the finite element model using nodal field recovery, the flux density on-axis is not readily distinguishable from the graph shown in figure 2. However, the integral under this curve differs from the Biot-Savart evaluation by about 0.5%.

Figures 5 and 6 respectively show:

- the computed Biot-Savart flux density on the plane Z=-0.9 metres inside the tank
- the difference between this and the values computed using nodal fields

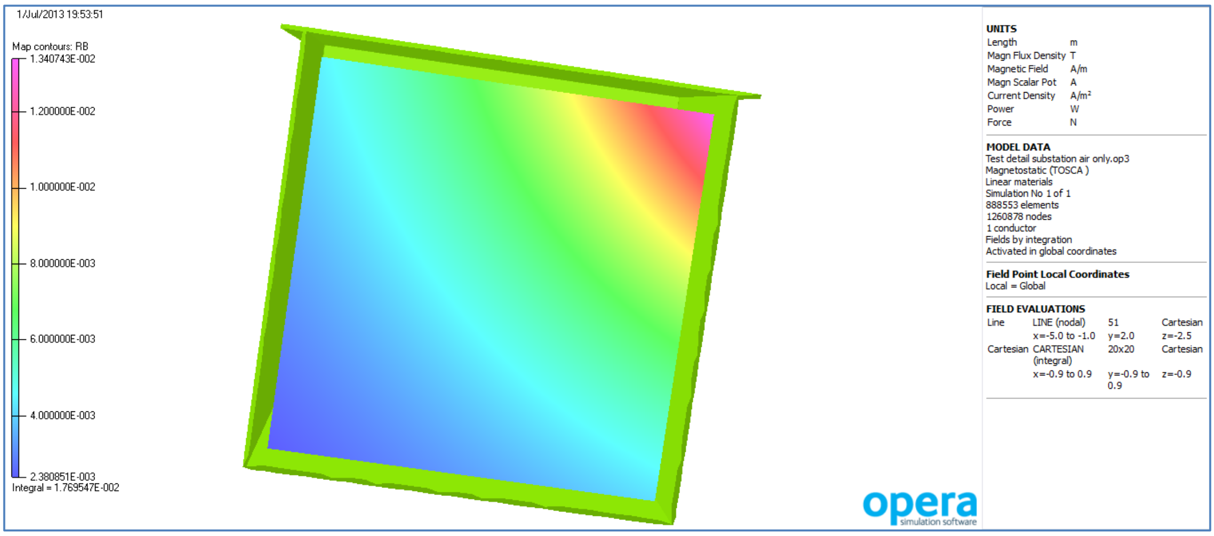

```
UNITS
Length              m
Magn Flux Density   T
Magnetic Field      A/m
Magn Scalar Pot     A
Current Density     A/m²
Power               W
Force               N

MODEL DATA
Test detail substation air only.op3
Magnetostatic (TOSCA )
Linear materials
Simulation No 1 of 1
888553 elements
1260878 nodes
1 conductor
Fields by integration
Activated in global coordinates

Field Point Local Coordinates
Local = Global

FIELD EVALUATIONS
Line       LINE (nodal)      51          Cartesian
           x=-5.0 to -1.0    y=2.0       z=-2.5
Cartesian  CARTESIAN         20x20       Cartesian
           (integral)
           x=-0.9 to 0.9     y=-0.9 to   z=-0.9
                             0.9
```

Figure 5: Flux density inside tank at Z = -0.9 metres computed using Biot-Savart

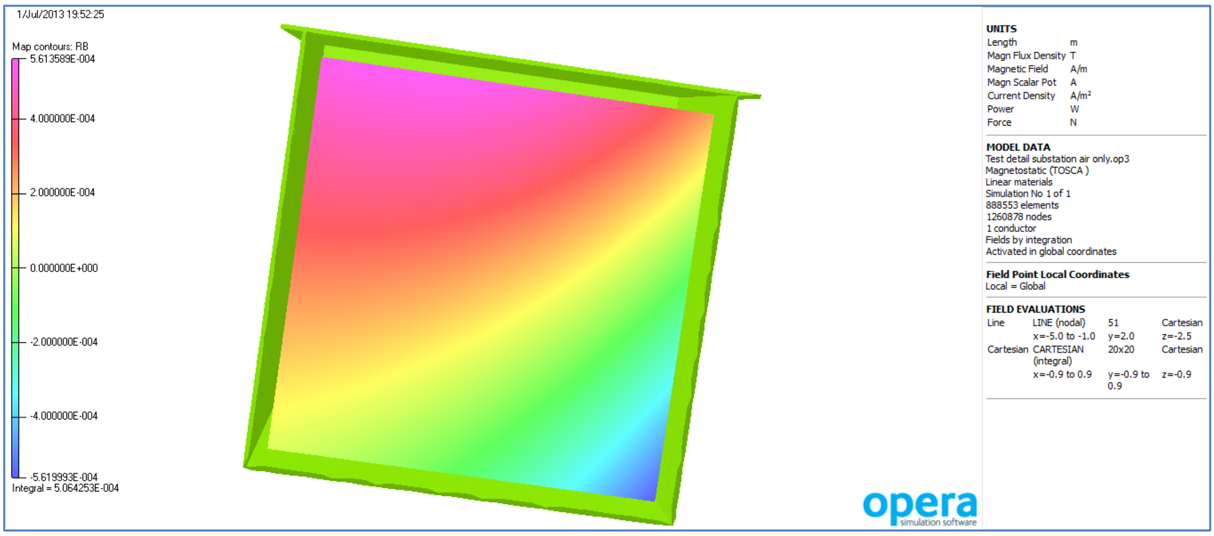

```
UNITS
Length              m
Magn Flux Density   T
Magnetic Field      A/m
Magn Scalar Pot     A
Current Density     A/m²
Power               W
Force               N

MODEL DATA
Test detail substation air only.op3
Magnetostatic (TOSCA )
Linear materials
Simulation No 1 of 1
888553 elements
1260878 nodes
1 conductor
Fields by integration
Activated in global coordinates

Field Point Local Coordinates
Local = Global

FIELD EVALUATIONS
Line       LINE (nodal)      51          Cartesian
           x=-5.0 to -1.0    y=2.0       z=-2.5
Cartesian  CARTESIAN         20x20       Cartesian
           (integral)
           x=-0.9 to 0.9     y=-0.9 to   z=-0.9
                             0.9
```

Figure 6: Difference between Biot-Savart and nodal fields all AIR model at Z = -0.9 metres

As shown in figure 5, the flux density on this plane varies between 2.4 and 13.4 mT, while figure 6 shows that the effect of the finite element mesh on the accuracy is approximately ±0.6 mT maximum. Consequently, when the substructure model of the substation is examined, it should be borne in mind that differences seen between the "real" model and the substructure model below this level may not be relied on.

Recommendation 1 for MICE Hall model: The effect of solving the magnetic fields in free space using a truncated finite element mesh appears to give about an average 5% error in the "far field" in the test model. The error will be smaller closer to the solenoid coils and larger near the boundary of the model. This inherent error from using finite elements should be considered when making judgements about maximum flux density levels in critical areas of the MICE Hall by repeating this

type of calculation for the complete MICE Hall model and investigating the error in the volume where a substructure model is required.

Simplified Substation Models

3 simplified models of the substation have been considered:

- Tank wall only made from mild steel (see figure 7)
- Tank wall and central 1010 steel volume equivalent to volume of transformer yoke and steel for instrument cabinet. (The volume of mild steel in the instrument cabinet is very small – hence the decision to use the 1010 steel BH curve.) (see figure 8)
- Tank wall with interior filled with a ferrous material using a dilute BH curve (see figure 9)

In all cases, the tank has also been simplified such that the lid is the same dimension in X and Z as the tank (2 x 2 metres). Figures 7 through 9 show the geometry of these models (with faces removed to show interior structure).

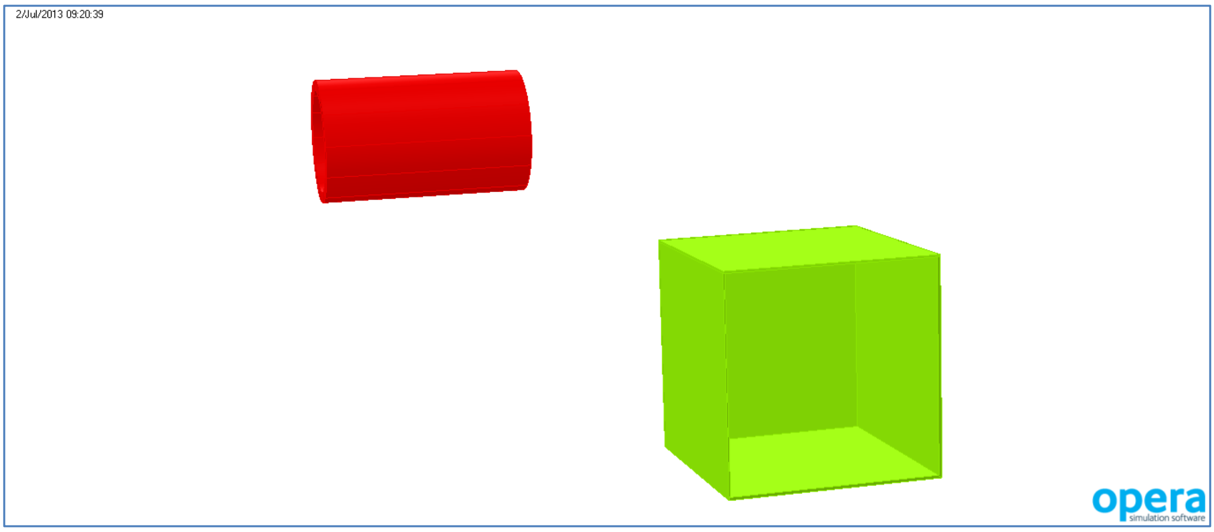

Figure 7: Empty tank

Each model has also been solved with 2 levels of discretization – maximum element size in simplified substation and immediate surrounding air is 0.2 metres or 0.5 metres.

The dilute BH characteristic for the example shown in figure 9 was determined by using a scaling factor

(volume of yoke + volume of instrument cabinet) / (volume of interior of tank)

applied to the magnetization of the 1010 material curve. This gives the BH curve shown in figure 10. In this model the dilution factor is 0.089 (8.9%)

Finding a method to assess these different models is not obvious. Clearly, the flux density values inside the tank will be different from the "real" model containing the yoke and the instrument cabinet – so comparison is not meaningful. Also, the flux density values inside the tank are small compared to the source field due to the shielding action of the tank wall.

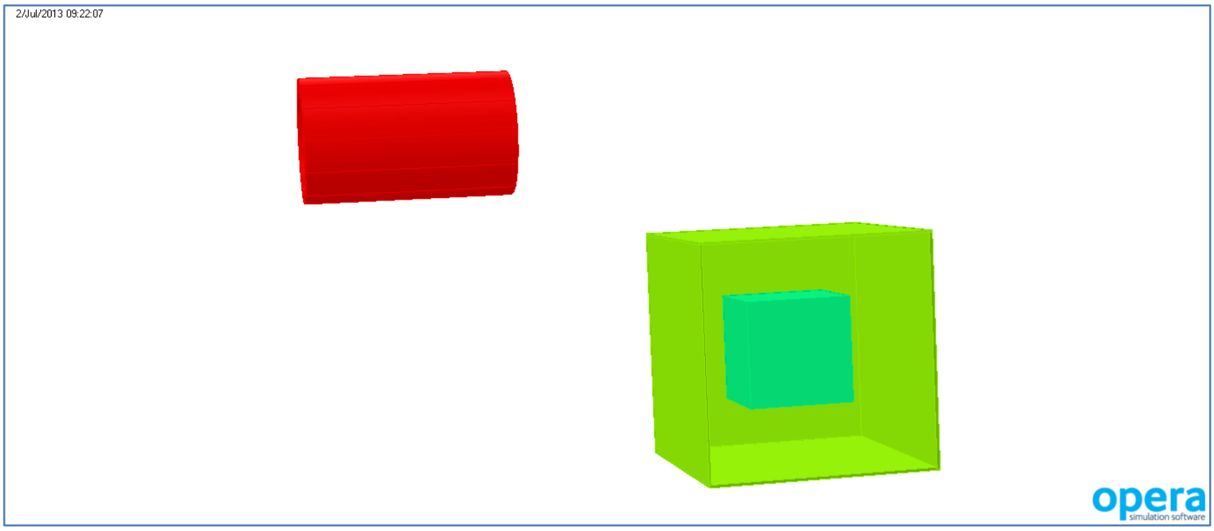

Figure 8: Tank and equivalent steel volume

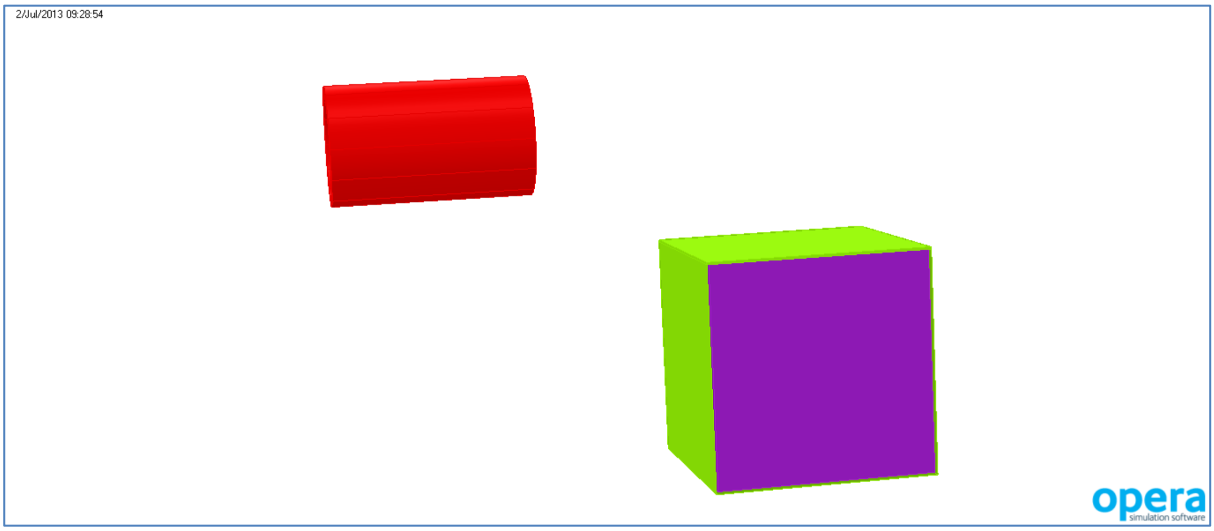

Figure 9: Tank and dilute ferrous volume

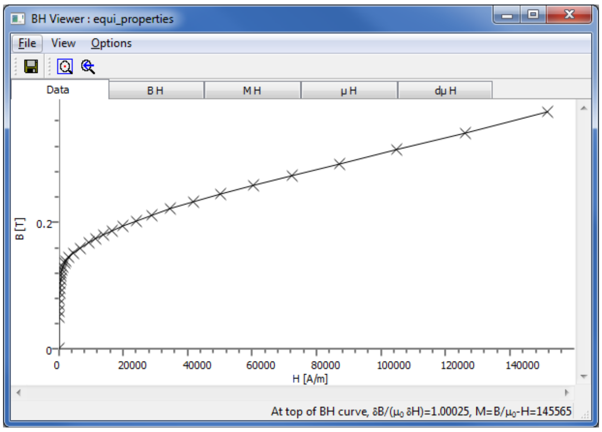

At top of BH curve, $\delta B/(\mu_0\,\delta H)=1.00025$, $M=B/\mu_0-H=145565$

Figure 10: Diluted BH curve

So a better method to assess the best model for a simplified structure is to examine the field distribution outside the substation. Figures 11 through 17 show the flux density on the surface of the air cell surrounding the substation for the “real” model and for the simplified structures.

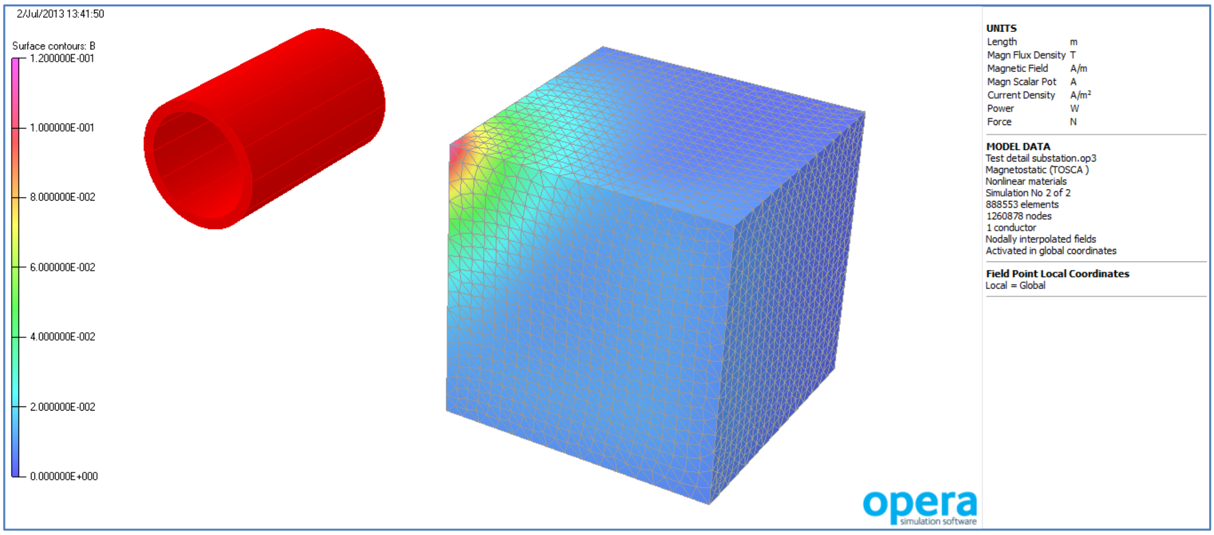

Figure 11: Magnitude of flux density on air cell surrounding "real" substation model

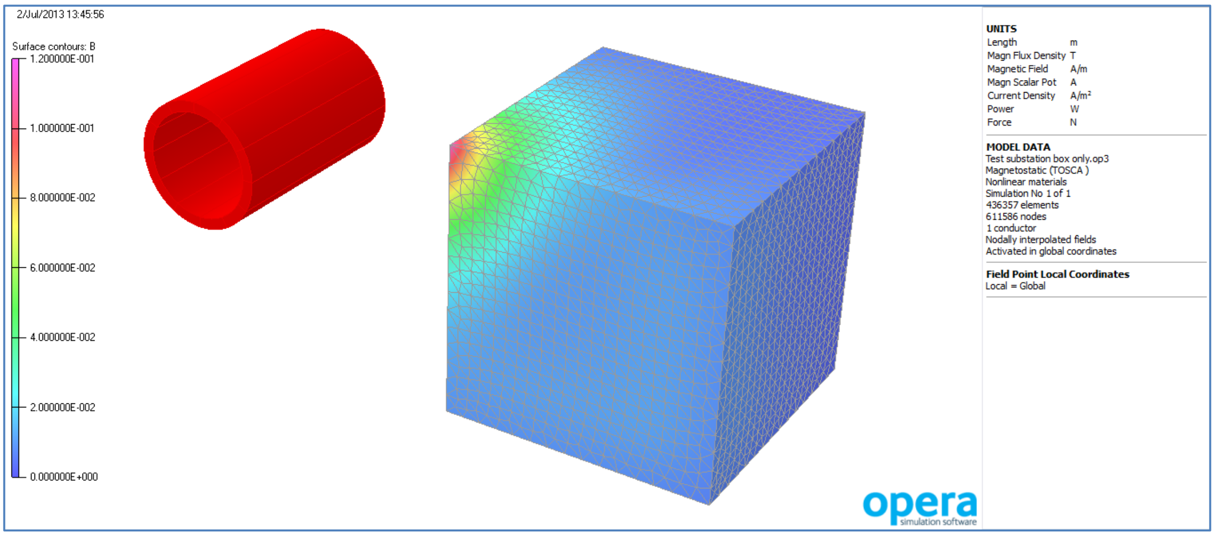

Figure 12: Magnitude of flux density on air cell surrounding tank only substation model 0.2 metre elements

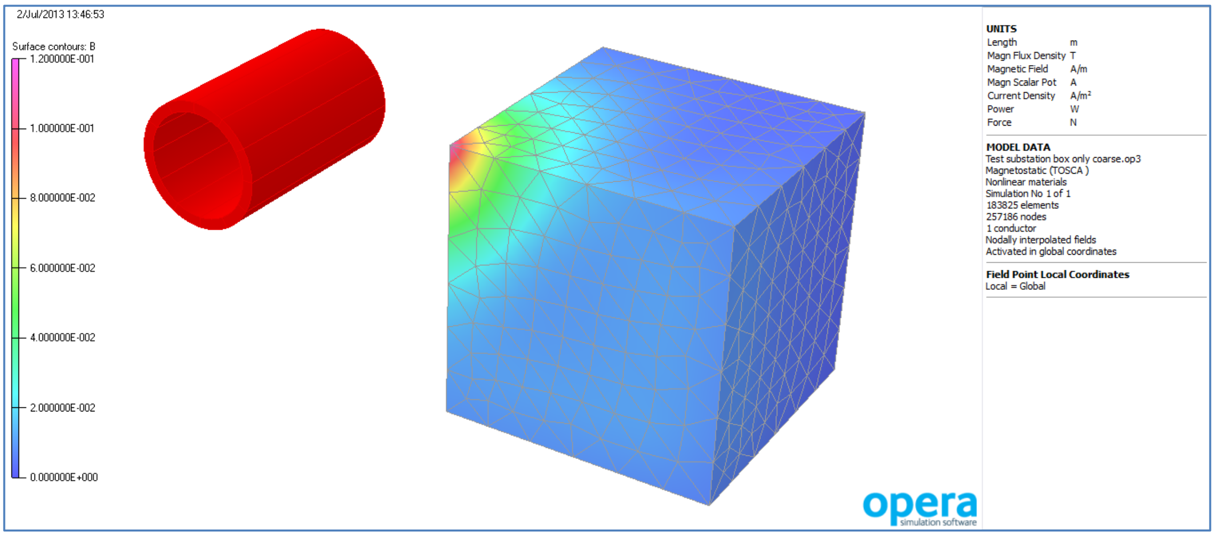

Figure 13: Magnitude of flux density on air cell surrounding tank only substation model 0.5 metre elements

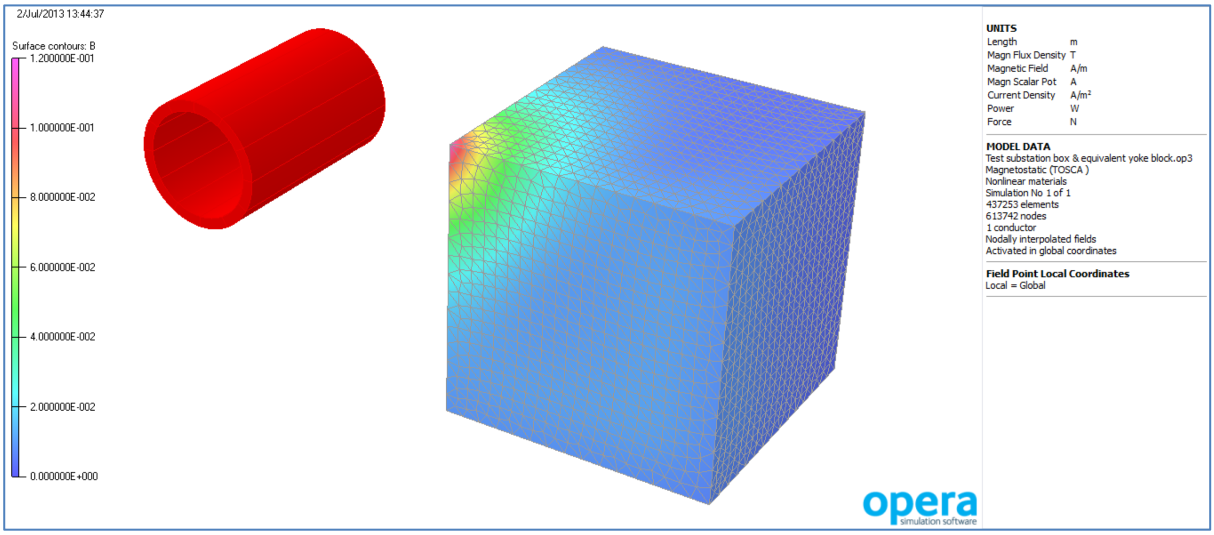

UNITS

Length	m
Magn Flux Density	T
Magnetic Field	A/m
Magn Scalar Pot	A
Current Density	A/m²
Power	W
Force	N

MODEL DATA
Test substation box & equivalent yoke block.op3
Magnetostatic (TOSCA)
Nonlinear materials
Simulation No 1 of 1
437253 elements
613742 nodes
1 conductor
Nodally interpolated fields
Activated in global coordinates

Field Point Local Coordinates
Local = Global

Figure 14: Magnitude of flux density on air cell surrounding tank and equivalent volume 1010 block substation model 0.2 metre elements

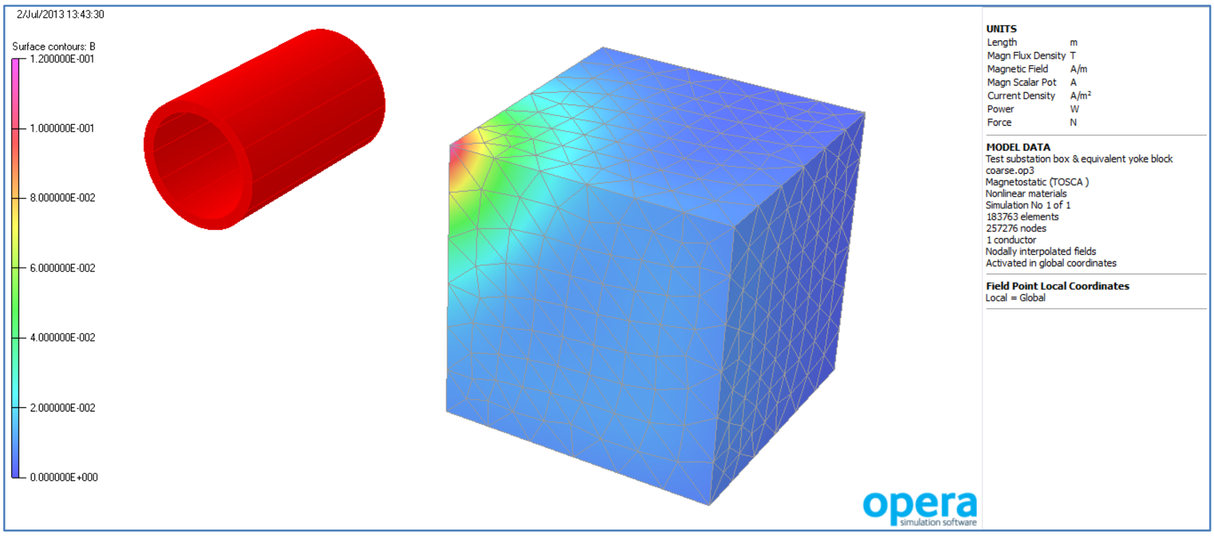

UNITS

Length	m
Magn Flux Density	T
Magnetic Field	A/m
Magn Scalar Pot	A
Current Density	A/m²
Power	W
Force	N

MODEL DATA
Test substation box & equivalent yoke block coarse.op3
Magnetostatic (TOSCA)
Nonlinear materials
Simulation No 1 of 1
183763 elements
257276 nodes
1 conductor
Nodally interpolated fields
Activated in global coordinates

Field Point Local Coordinates
Local = Global

Figure 15: Magnitude of flux density on air cell surrounding tank and equivalent volume 1010 block substation model 0.5 metre elements

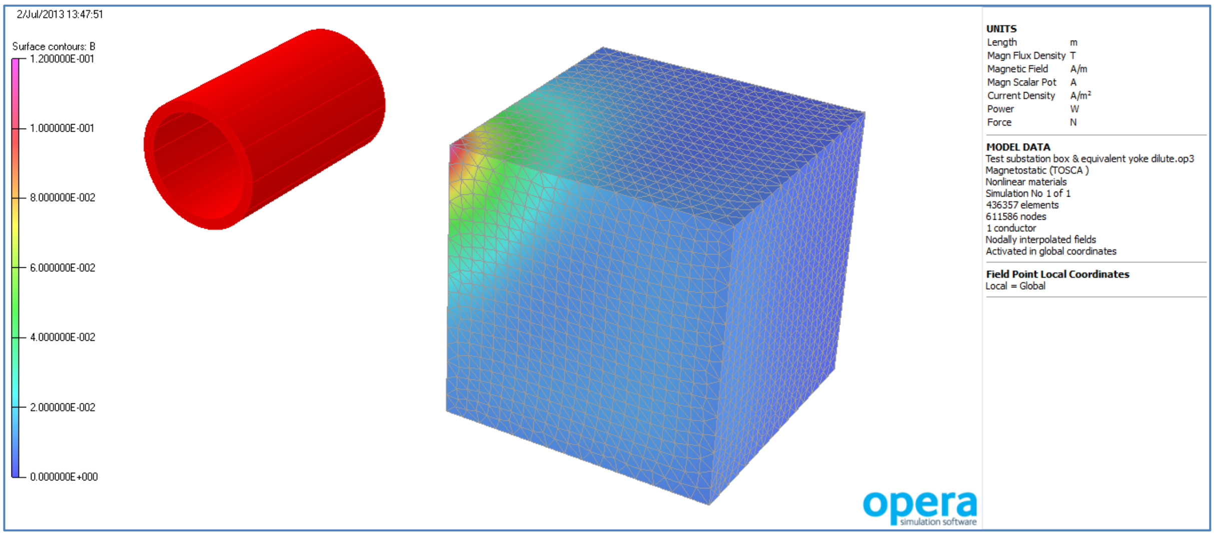

UNITS

Length	m
Magn Flux Density	T
Magnetic Field	A/m
Magn Scalar Pot	A
Current Density	A/m²
Power	W
Force	N

MODEL DATA
Test substation box & equivalent yoke dilute.op3
Magnetostatic (TOSCA)
Nonlinear materials
Simulation No 1 of 1
436357 elements
611586 nodes
1 conductor
Nodally interpolated fields
Activated in global coordinates

Field Point Local Coordinates
Local = Global

Figure 16: Magnitude of flux density on air cell surrounding tank and filled dilute material substation model 0.2 metre elements

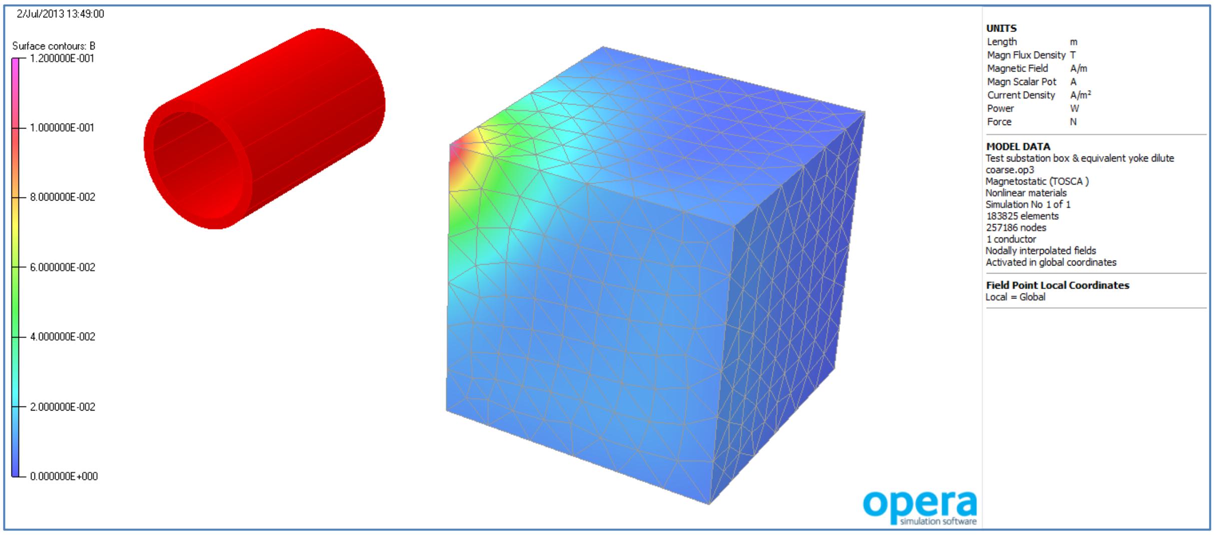

Figure 17: Magnitude of flux density on air cell surrounding tank and filled dilute material substation model 0.5 metre elements

As can be seen, from a visual inspection point of view, there is little difference between the "real" model flux density at this surface and all of the simplified substation models. Table 1 gives a better insight, however. This shows the surface integral of the magnitude of the flux density on the same surface and the difference between the integral for the simplified models and the "real" model

Table 1: Surface integral of flux density on air surrounding substation

Model	Element size (m)	Surface integral (T - m²)	% difference
"Real" model	-	0.5130	-
Tank only	0.2	0.5134	+0.08
	0.5	0.5123	-0.14
Tank and equivalent volume of 1010 steel	0.2	0.5135	+0.10
	0.5	0.5124	-0.12
Tank and filled dilute material	0.2	0.5164	+0.66
	0.5	0.5152	+0.43

There are two very obvious conclusions that can be drawn from this table:

- The tank and dilute material option is the poorest simplified representation
- There is little to choose between representing the substation as a hollow tank and as a tank containing an equivalent amount of 1010 steel

It can also be seen that element size, for both the simplified hollow tank and the simplified tank containing an equivalent amount of steel, does not make that much difference.

Recommendation 2 for MICE Hall model: Structure inside the MICE Hall that consists of a steel outer "cabinet" with internal ferromagnetic structure can be adequately simplified to either a hollow structure of approximately the same dimensions as the outer cabinet, or an approximate cabinet with a single, appropriately dimensioned, ferromagnetic block placed at its centre. If the existing model includes structure where the block is already in place, don't bother to remove it. But, if future cabinets are added, the outer cabinet should be sufficient to get source fields for a detailed substructure model.

Recommendation 3 for MICE Hall model: Element size in the free space surrounding a substructure should not need to be reduced to the level that may be needed for a detailed substructure model in order to adequately capture the source field from the complete MICE Hall model

Substructure models

In this section, the field obtained from the simplified substation models is used as a source field to a detailed substructure model of the substation. This is then compared to the model of the "real" substation.

As shown in table 1, there is little difference between the tank alone and the tank with equivalent volume models. Consequently, the substructure models are tested with:

- the 0.2 metre element discretization for the tank with equivalent volume model
- the 0.5 metre element discretization of the tank alone model

These tests were to reinforce the recommendations 2 and 3 above.

Figure 18 shows the full extent of the substructure model – a 1.5 x 1.5 x 1.5 metre cube surrounding the detail model of the substation used in the "real" model. In this study, all the air is set as reduced potential so that the field results from the simplified substation models can be used as source fields in the substructure model. The extracted fields are imported as a vector, RHS, and the external boundary is set as a normal magnetic boundary condition.

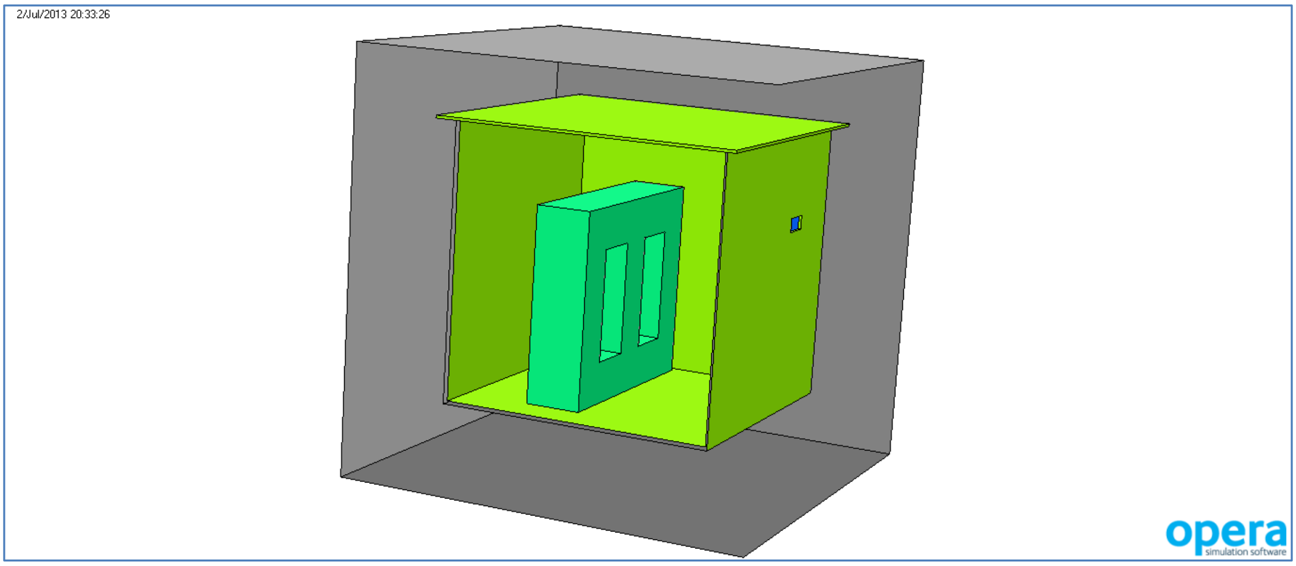

Figure 18: Geometry of detailed substructure model to which source fields are imported

Figure 19 shows the magnetic field on the plane at Z = -0.9 metres inside the substructure model using source fields imported from the 0.2 metre element tank with equivalent volume model. Figure 20 shows the same for source fields imported from the 0.5 metre element tank only model. Both field maps are in the range 0.5 to 3.0 mT. There are some differences in the solution, but these are within the range -0.25 to +0.1 mT, as shown in figure 21. This difference is less than the ±0.6 mT maximum error associated with the use of a finite element method (see earlier air only model). Note that figure 20 also shows that the increased element size for the tank only model source fields is reflected in the substructure model, giving the slightly "ragged" look.

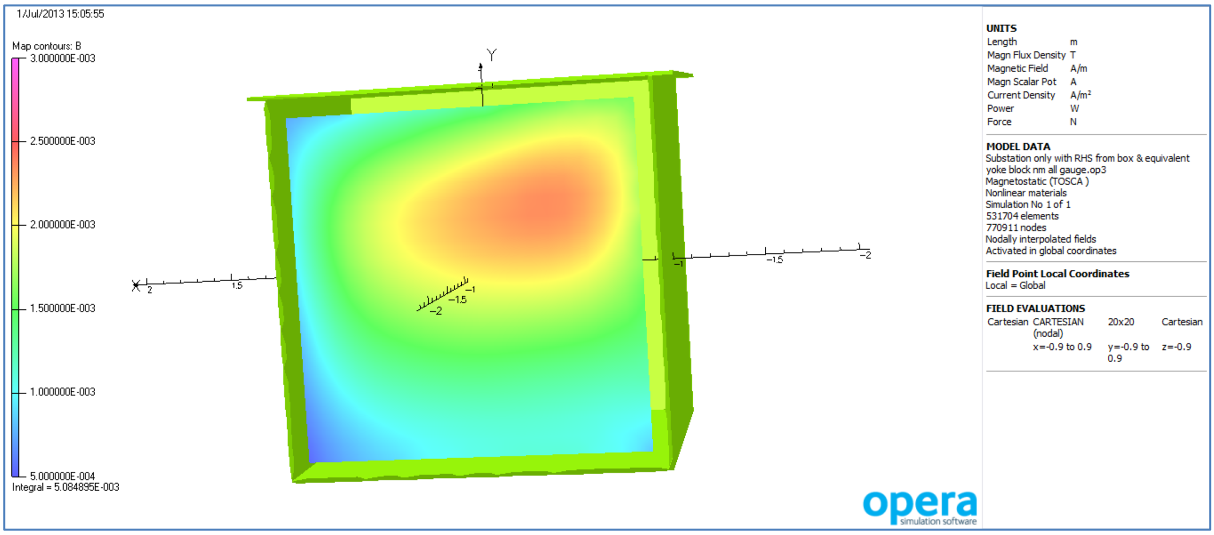

Figure 19: Fields on plane Z = -0.9 metres in substructure model with imported source from 0.2 metre element tank with equivalent 1010 volume model

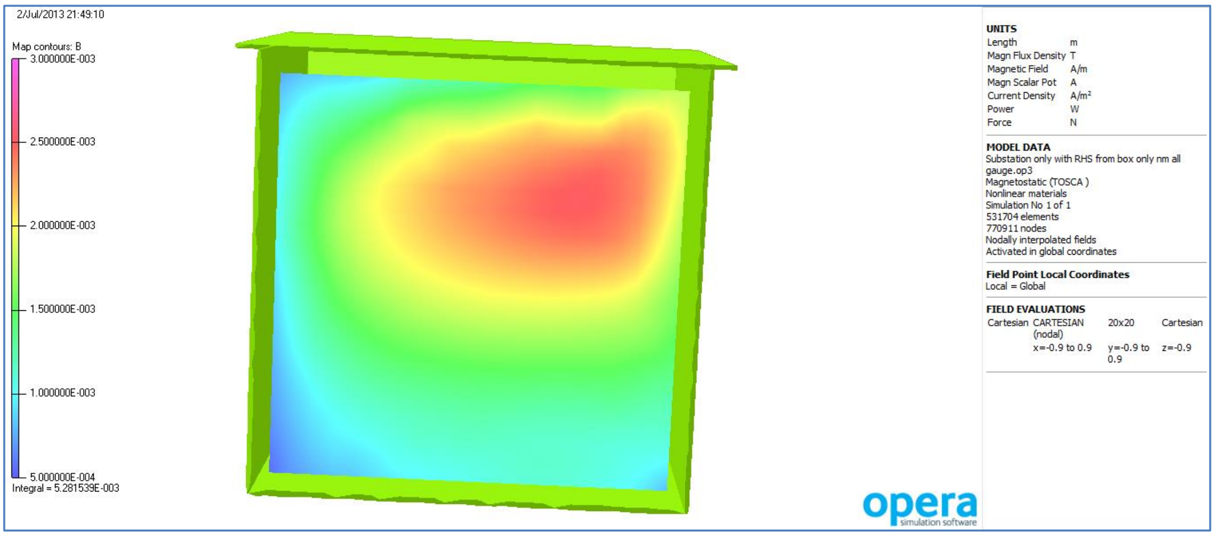

Figure 20: Fields on plane Z = -0.9 metres in substructure model with imported source from 0.5 metre element tank only model

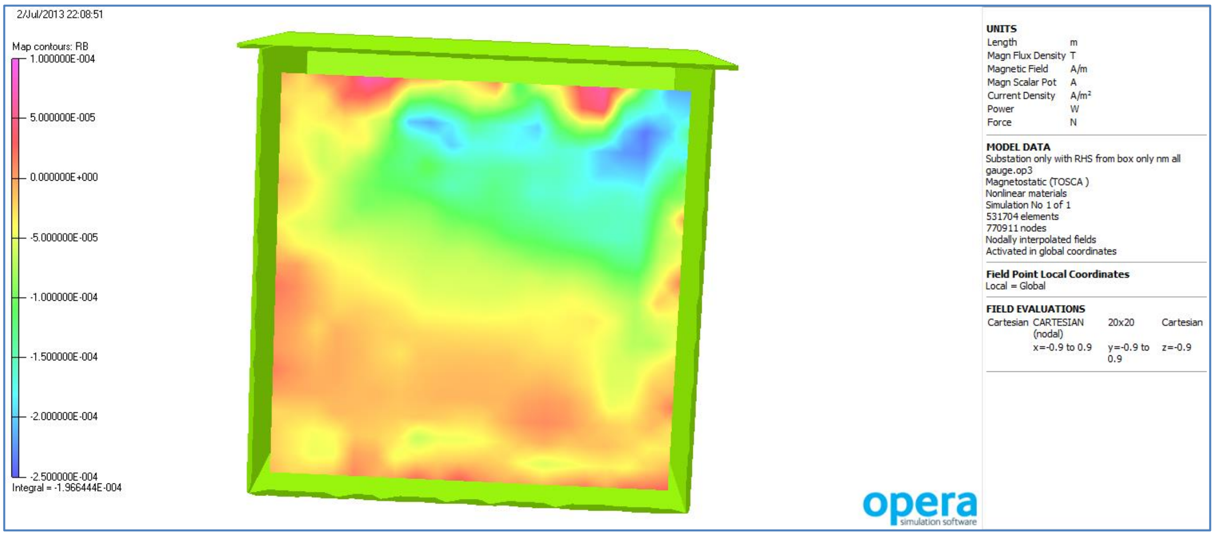

Figure 21: Difference in flux density at Z = -0.9 in substructure models

Figure 22 shows the magnetic field on the plane Z = -0.9 metres in the “real” model (solved with the actual solenoid). It can be seen that this is quite similar to the substructure models, but the peak fields are somewhat higher. This difference can be seen in figures 23 and 24, which compare the values in the “real” model with the values in the substructure model using the source fields from the 0.2 metre element tank and equivalent 1010 volume model and the 0.5 metre element tank only model respectively. The field maps for both figures are in the range 0 to 0.5 mT.

The results in figures 23 and 24 show that, if anything, recovering source fields from the tank only model with 0.5 metre elements actually produces results that are closer to the “real” model than using the 0.2 metre element model with the tank and equivalent 1010 volume over most of the mapped region. However, again the differences for both are within the ±0.6 mT difference associated with using the finite element model – so either simplified model for the substation is acceptable.

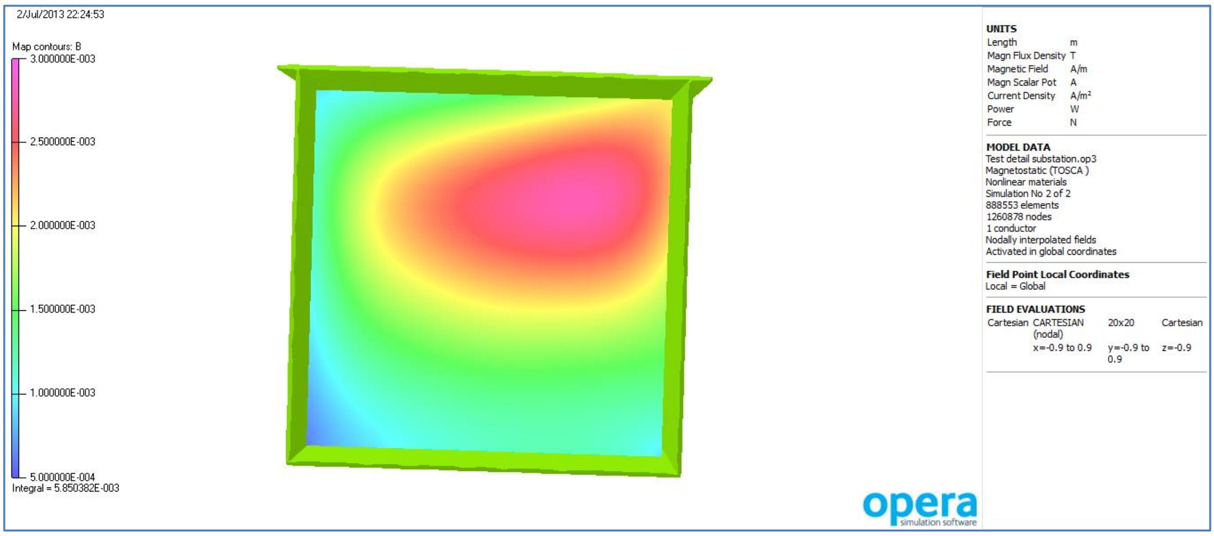

UNITS
Length m
Magn Flux Density T
Magnetic Field A/m
Magn Scalar Pot A
Current Density A/m²
Power W
Force N

MODEL DATA
Test detail substation.op3
Magnetostatic (TOSCA)
Nonlinear materials
Simulation No 2 of 2
888553 elements
1260878 nodes
1 conductor
Nodally interpolated fields
Activated in global coordinates

Field Point Local Coordinates
Local = Global

FIELD EVALUATIONS
Cartesian CARTESIAN (nodal) 20x20 Cartesian
x=-0.9 to 0.9 y=-0.9 to 0.9 z=-0.9

Figure 22: Fields on plane Z = -0.9 metres in “real” model

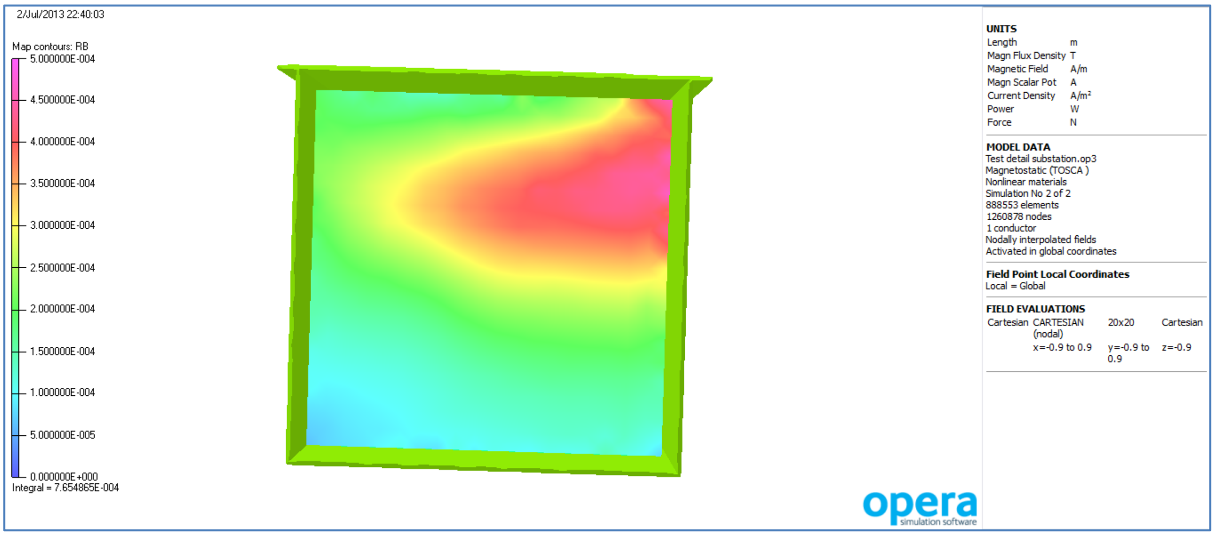

UNITS
Length m
Magn Flux Density T
Magnetic Field A/m
Magn Scalar Pot A
Current Density A/m²
Power W
Force N

MODEL DATA
Test detail substation.op3
Magnetostatic (TOSCA)
Nonlinear materials
Simulation No 2 of 2
888553 elements
1260878 nodes
1 conductor
Nodally interpolated fields
Activated in global coordinates

Field Point Local Coordinates
Local = Global

FIELD EVALUATIONS
Cartesian CARTESIAN (nodal) 20x20 Cartesian
x=-0.9 to 0.9 y=-0.9 to 0.9 z=-0.9

Figure 23: Difference in flux density at Z = -0.9 between “real” model and substructure model with source field from tank and equivalent 1010 volume model

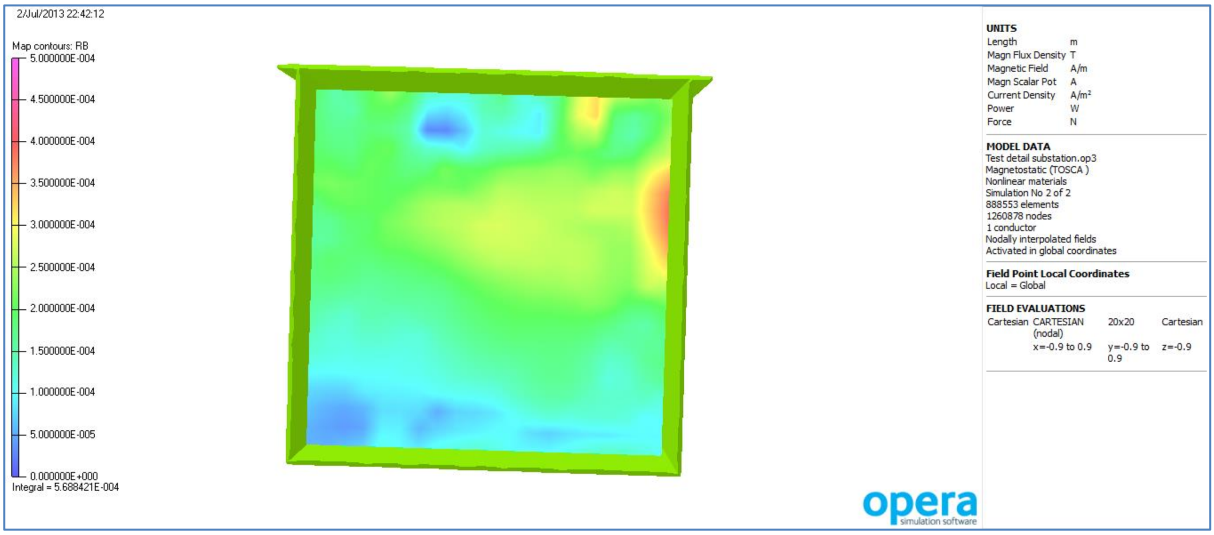

Figure 24: Difference in flux density at Z = -0.9 metres between “real” model and substructure model with source field from tank only model

These results from these models do reinforce recommendations 2 and 3, but also show that the results obtained using source fields from simplified models in a substructure could be different by a maximum of about 20% of the flux density that would be obtained if a detailed model of a substation (or similar) could be included in the overall MICE Hall model. Generally, however, the differences will probably be below 10%. These differences should also be compared to the differences that are inherent in the finite element modelling to assess if they are significant.

Shielding Wall Model

Effect of finite element discretization

As with the substation, the effect of the discretization of the “real” wall model compared to the Biot-Savart expression calculation of the source fields has been determined. Consequently, the “real” wall model has been run with all the materials set with AIR properties and total potential.

Figures 25 and 26 show the Biot-Savart calculation of the field on two 10 x 6 metre planes at Z = +0.5 and Z = +1.0 metres respectively. Note that the I-beams end at Z = +0.25 metres – that is the two planes are 0.25 and 0.75 metres behind the shielding wall I-beams respectively.

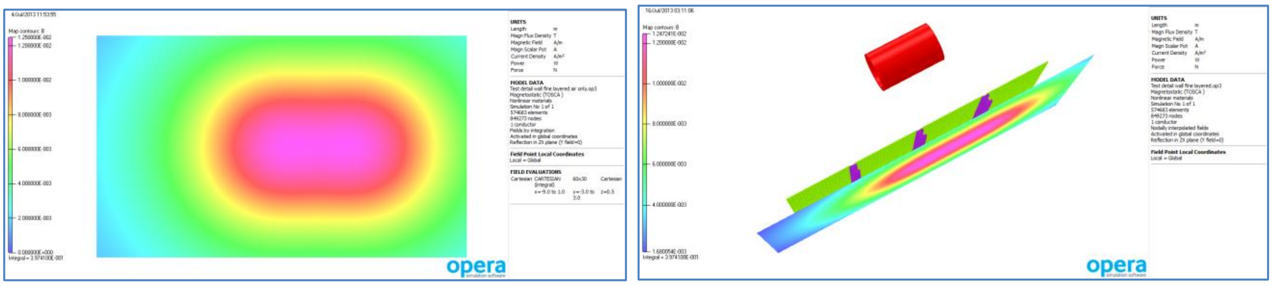

Figure 25: Flux density computed from Biot-Savart expression at Z = 0.5 metres

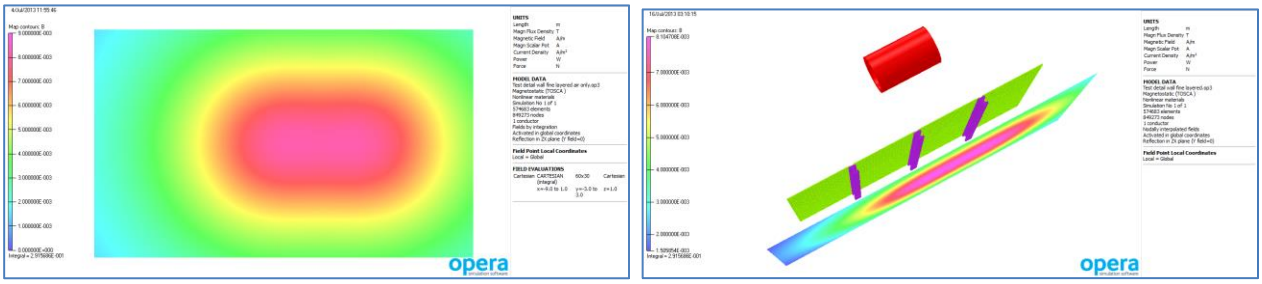

UNITS

Length	m
Magn Flux Density	T
Magnetic Field	A/m
Magn Scalar Pot	A
Current Density	A/m²
Power	W
Force	N

MODEL DATA
Test detail wall fine layered air only.op3
Magnetostatic (TOSCA)
Nonlinear materials
Simulation No 1 of 1
574683 elements
849273 nodes
1 conductor
Fields by integration
Activated in global coordinates
Reflection in ZX plane (Y field=0)

Field Point Local Coordinates
Local = Global

FIELD EVALUATIONS
Cartesian CARTESIAN (integral) 60x30 Cartesian
x=-9.0 to 1.0 y=-3.0 to 3.0 z=1.0

UNITS

Length	m
Magn Flux Density	T
Magnetic Field	A/m
Magn Scalar Pot	A
Current Density	A/m²
Power	W
Force	N

MODEL DATA
Test detail wall fine layered.op3
Magnetostatic (TOSCA)
Nonlinear materials
Simulation No 1 of 1
574683 elements
849273 nodes
1 conductor
Nodally interpolated fields
Activated in global coordinates
Reflection in ZX plane (Y field=0)

Field Point Local Coordinates
Local = Global

Figure 26: Flux density computed from Biot-Savart expression at Z = 1.0 metres

Figures 27 and 28 show the difference between the values computed in the finite element mesh of the free space model using nodal field recovery and the Biot-Savart calculated fields. As will be discussed in the next section, the "real" wall model has been run with 3 different levels of discretization. For this comparison, the third of these (smallest elements + 2 layers in the wall) was chosen for the free space model.

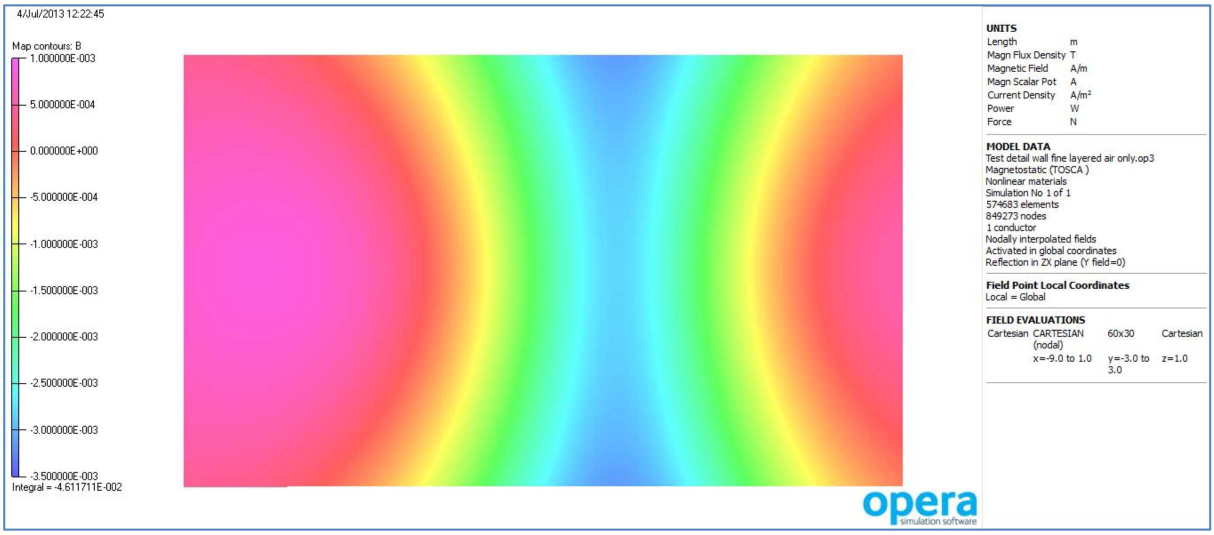

UNITS

Length	m
Magn Flux Density	T
Magnetic Field	A/m
Magn Scalar Pot	A
Current Density	A/m²
Power	W
Force	N

MODEL DATA
Test detail wall fine layered air only.op3
Magnetostatic (TOSCA)
Nonlinear materials
Simulation No 1 of 1
574683 elements
849273 nodes
1 conductor
Nodally interpolated fields
Activated in global coordinates
Reflection in ZX plane (Y field=0)

Field Point Local Coordinates
Local = Global

FIELD EVALUATIONS
Cartesian CARTESIAN (nodal) 60x30 Cartesian
x=-9.0 to 1.0 y=-3.0 to 3.0 z=1.0

Figure 27: Difference in flux density between Biot-Savart and nodal field recovery at Z = 0.5 metres

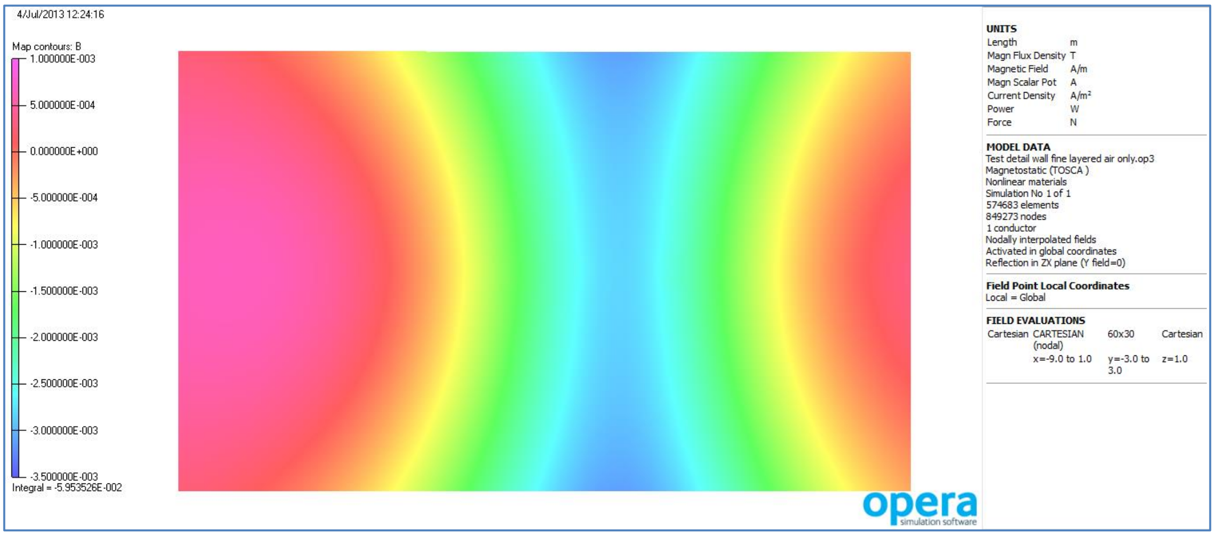

UNITS

Length	m
Magn Flux Density	T
Magnetic Field	A/m
Magn Scalar Pot	A
Current Density	A/m²
Power	W
Force	N

MODEL DATA
Test detail wall fine layered air only.op3
Magnetostatic (TOSCA)
Nonlinear materials
Simulation No 1 of 1
574683 elements
849273 nodes
1 conductor
Nodally interpolated fields
Activated in global coordinates
Reflection in ZX plane (Y field=0)

Field Point Local Coordinates
Local = Global

FIELD EVALUATIONS
Cartesian CARTESIAN (nodal) 60x30 Cartesian
x=-9.0 to 1.0 y=-3.0 to 3.0 z=1.0

Figure 28: Difference in flux density between Biot-Savart and nodal field recovery at Z = 1.0 metres

It can be seen that the maximum difference between the Biot-Savart and nodal field is about 3 mT, compared to maximum fields of 12.5 mT at Z=0.5 metres and 9 mT at Z=1.0 metres. These differences of up to 30% primarily occur because of an implied image of the source in the nodal field models. The outer boundary of the model in the direction of the wall is at Z=4.0 metres and the axis of the solenoid is at Z=-2.5

metres – which implies that there is a second source at Z=10.5 metres (and further implied images after that). When assessing the effectiveness of the shields, this level of difference should be born in mind.

Recommendation 4 for MICE Hall model: When trying to examine the shielding effect supplied by magnetic walls, the outer boundary of the model should be made as large as practically possible to avoid image sources.

“Real” wall models

The model with the “real” wall has been analysed with 3 levels of discretization:

1. 0.25 metre prism elements in the X and Y directions, 1 layer of elements in the thickness of the wall panels
2. 0.1 metre prism elements in the X and Y directions, 1 layer of elements in the thickness of the wall panels
3. 0.1 metre prism elements in the X and Y directions, 2 layers of elements in the thickness of the wall panels

There are also corresponding discretization changes in the size of prism elements in the Y-direction I-beam such that they match with the elements in the panels.

Figures 29 through 34 show the flux density on the same planes at Z=0.5 and Z=1.0 metres for the 3 cases. As can be seen, there are no perceptible changes between the results for the 3 levels of discretization. As can be seen in figure 35, the flux density in the wall panels is effectively in-plane and varies reasonably slowly in X and Y despite the inclusion of the I-beams and gaps. Consequently, even the largest prism elements (0.25 x 0.25 x 0.01 metre) can capture the behaviour well.

Recommendation 5 for MICE Hall model: If substructure modelling of shielding walls is undertaken, the discretization of the wall and supports only needs to be at a reasonable level to capture the geometry. A fine mesh is not needed to capture variations in flux density as these will be small

The most interesting thing to note from these results is how poor the level of shielding is close to the solenoid. At Z = 0.5 metres, the maximum flux density is 8.5 mT compared to 12.5 mT calculated by the Biot-Savart expression (figure 25) and 15.5 mT calculated by the nodal averaging in the finite element mesh. At Z = 1 metre, the maximum flux density is about 5.75 mT compared to 9 to 12 mT in free space.

Of course, the reason for this is that the wall closest to the solenoid is quite highly saturated. As can be seen in figure 35, the maximum flux density is nearly 1.8 T. As a consequence, only about 50% shielding has been obtained in some areas.

Recommendation 6 for MICE Hall model: A quick way to assess how effective shielding will be – whether it is real shielding constructed for the purpose of reducing field or the outside cabinet of some equipment – is to determine where the steel is operating on the magnetic characteristic of the shielding material. Tangential components of magnetic field strength and the normal component of magnetic flux density will be continuous at the material surface, so this will also give an indication of the flux density just behind (or inside) the shielding wall

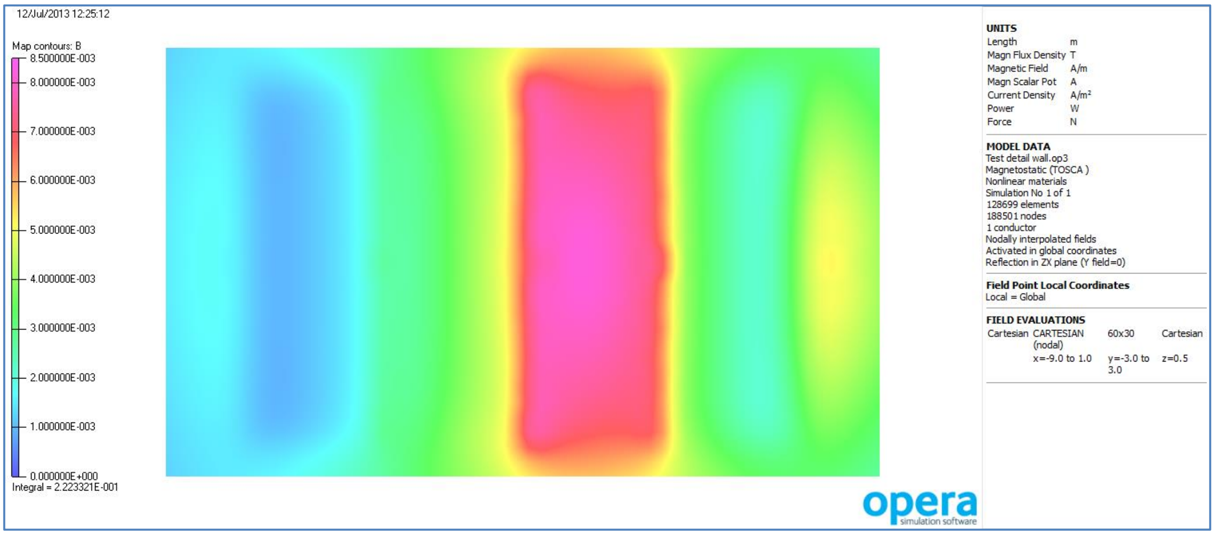

Figure 29: Flux density at Z = 0.5 metres with 0.25 metre elements and 1 layer

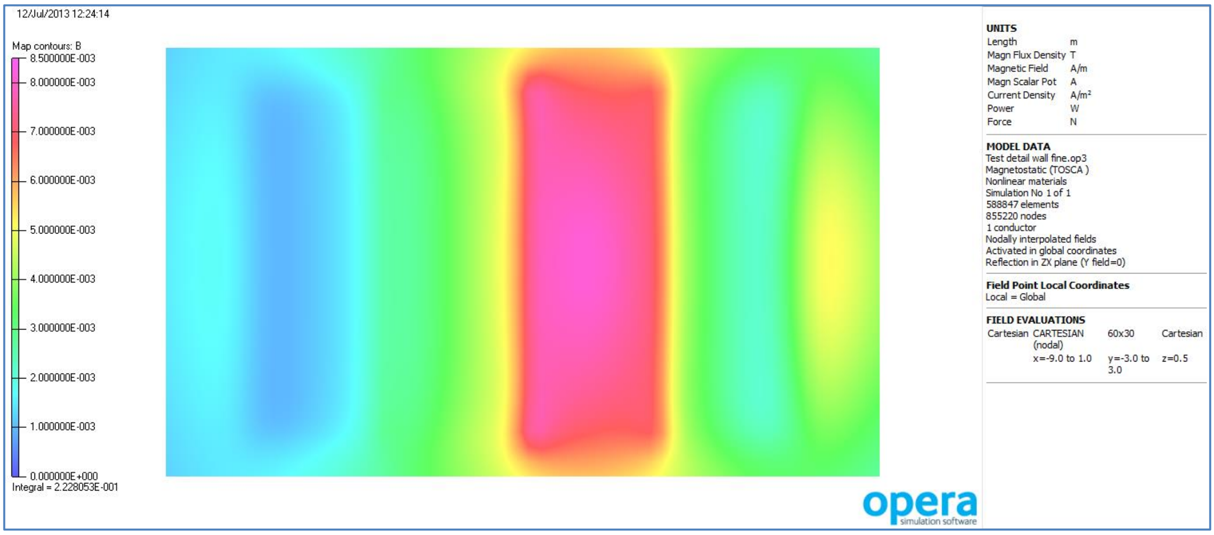

Figure 30: Flux density at Z = 0.5 metres with 0.1 metre elements and 1 layer

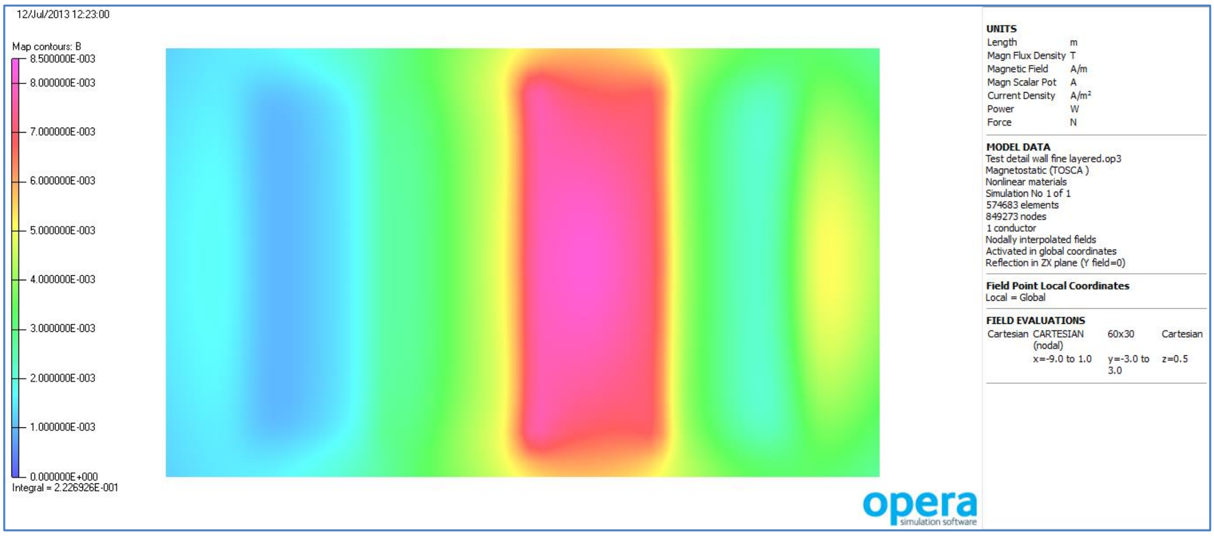

Figure 31: Flux density at Z = 0.5 metres with 0.1 metre elements and 2 layers

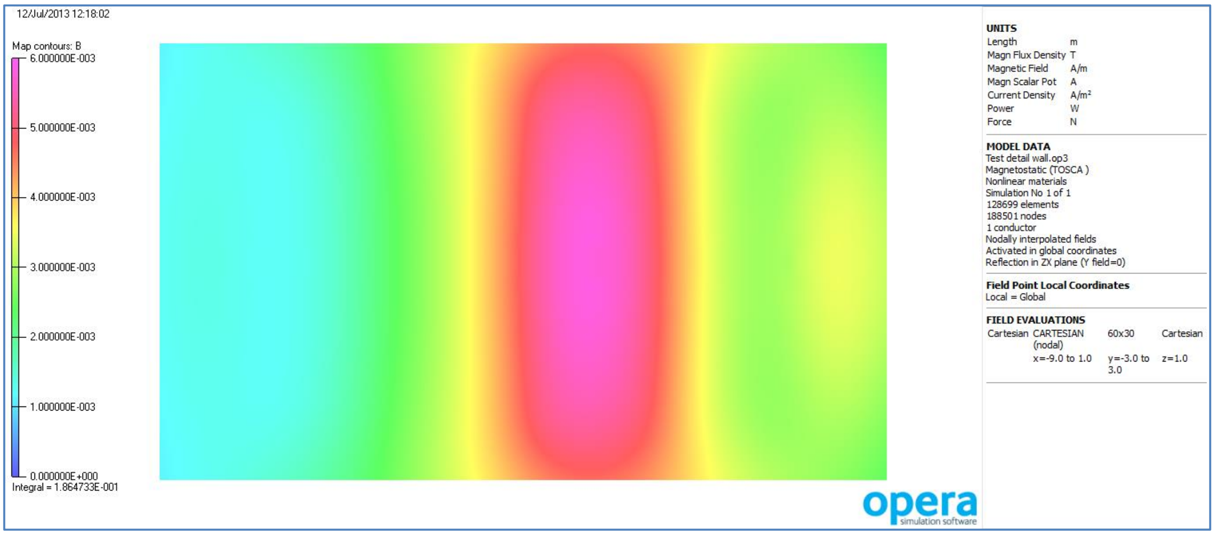

```
UNITS
Length              m
Magn Flux Density   T
Magnetic Field      A/m
Magn Scalar Pot     A
Current Density     A/m²
Power               W
Force               N

MODEL DATA
Test detail wall.op3
Magnetostatic (TOSCA )
Nonlinear materials
Simulation No 1 of 1
128699 elements
188501 nodes
1 conductor
Nodally interpolated fields
Activated in global coordinates
Reflection in ZX plane (Y field=0)

Field Point Local Coordinates
Local = Global

FIELD EVALUATIONS
Cartesian CARTESIAN       60x30          Cartesian
          (nodal)
          x=-9.0 to 1.0   y=-3.0 to      z=1.0
                          3.0
```

Figure 32: Flux density at Z = 1 metres with 0.25 metre elements and 1 layer

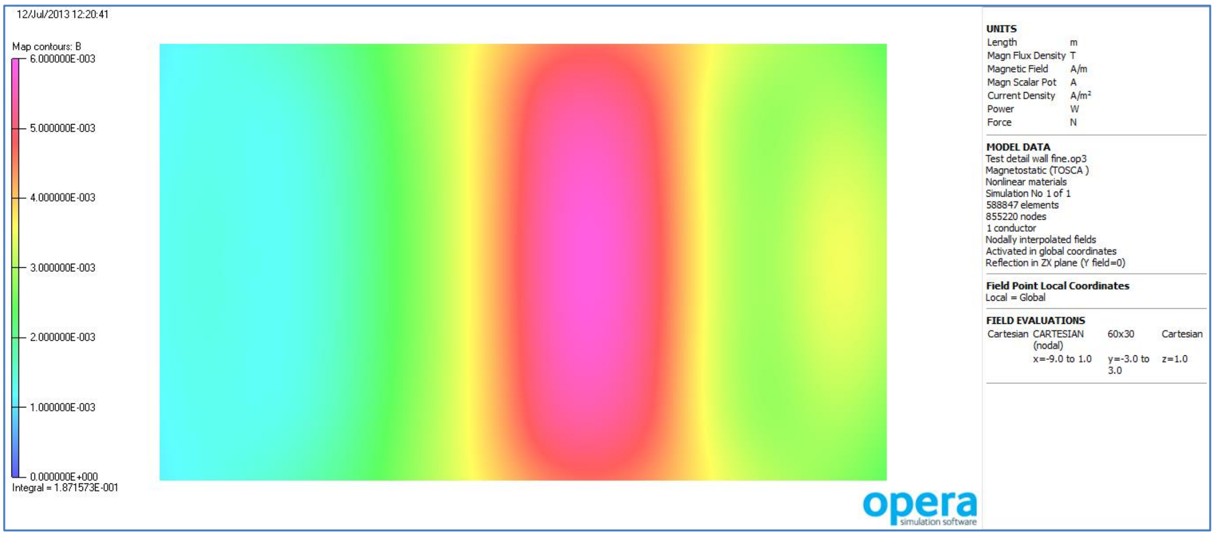

```
UNITS
Length              m
Magn Flux Density   T
Magnetic Field      A/m
Magn Scalar Pot     A
Current Density     A/m²
Power               W
Force               N

MODEL DATA
Test detail wall fine.op3
Magnetostatic (TOSCA )
Nonlinear materials
Simulation No 1 of 1
588847 elements
855220 nodes
1 conductor
Nodally interpolated fields
Activated in global coordinates
Reflection in ZX plane (Y field=0)

Field Point Local Coordinates
Local = Global

FIELD EVALUATIONS
Cartesian CARTESIAN       60x30          Cartesian
          (nodal)
          x=-9.0 to 1.0   y=-3.0 to      z=1.0
                          3.0
```

Figure 33: Flux density at Z = 1 metres with 0.1 metre elements and 1 layer

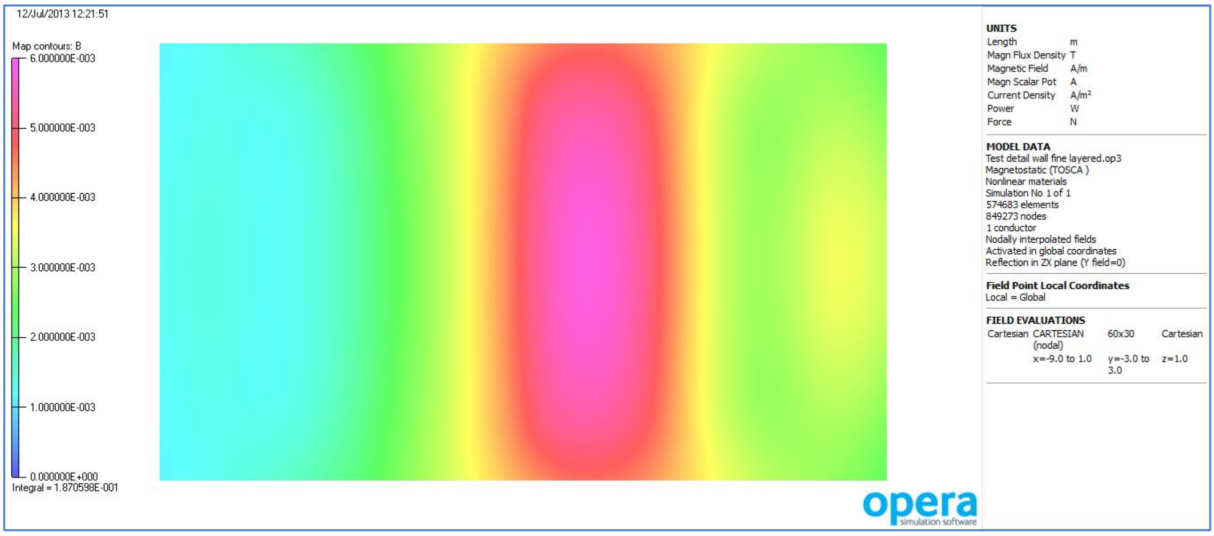

```
UNITS
Length              m
Magn Flux Density   T
Magnetic Field      A/m
Magn Scalar Pot     A
Current Density     A/m²
Power               W
Force               N

MODEL DATA
Test detail wall fine layered.op3
Magnetostatic (TOSCA )
Nonlinear materials
Simulation No 1 of 1
574683 elements
849273 nodes
1 conductor
Nodally interpolated fields
Activated in global coordinates
Reflection in ZX plane (Y field=0)

Field Point Local Coordinates
Local = Global

FIELD EVALUATIONS
Cartesian CARTESIAN       60x30          Cartesian
          (nodal)
          x=-9.0 to 1.0   y=-3.0 to      z=1.0
                          3.0
```

Figure 34: Flux density at Z = 1 metres with 0.1 metre elements and 2 layers

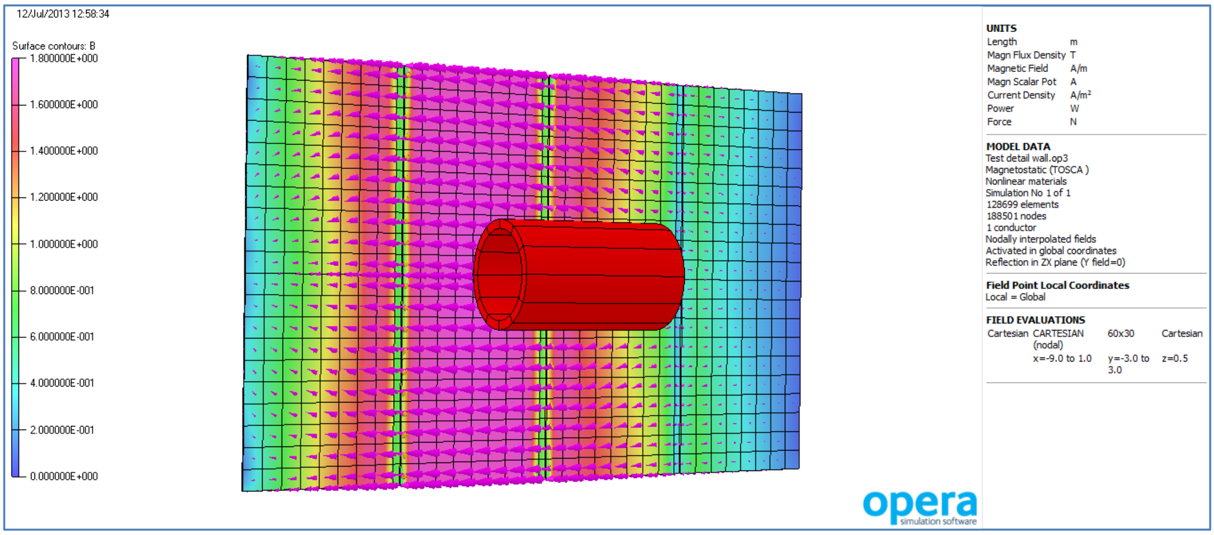

UNITS

Length	m
Magn Flux Density	T
Magnetic Field	A/m
Magn Scalar Pot	A
Current Density	A/m²
Power	W
Force	N

MODEL DATA
Test detail wall.op3
Magnetostatic (TOSCA)
Nonlinear materials
Simulation No 1 of 1
128699 elements
188501 nodes
1 conductor
Nodally interpolated fields
Activated in global coordinates
Reflection in ZX plane (Y field=0)

Field Point Local Coordinates
Local = Global

FIELD EVALUATIONS

Cartesian	CARTESIAN (nodal)	60x30	Cartesian
	x=-9.0 to 1.0	y=-3.0 to 3.0	z=0.5

Figure 35: Flux density in wall and I-beams with 0.25 metre elements and 1 layer

Comparison with simplified model

The "real" wall models are now compared to a simplified version of the wall. The overall dimensions of the wall panels are retained (7.9 x 5 x 0.025 metres) but it is treated as a single flat panel and the I-beams are omitted. Figure 36 shows the geometry and mesh (including the ZX plane replication).

The wall primarily consists of a single layer of prism elements of 0.25 x 0.25 metres or 0.1 x 0.25 metres. There are also some 0.05 x 0.25 metre prisms next to the 0.1 x 0.25 metre prisms. Figures 37 and 38 show the flux density on the Z = 0.5 and Z = 1.0 metre planes respectively.

Figures 39 and 40 show the difference between the simplified wall and the best discretized "real" wall results. As would be expected, the largest discrepancies occur at Z = 0.5 metres close to where the I-beams are situated. However, the maximum difference of about 1.3 mT is less than the 3 mT maximum difference seen in the finite element representation of the source fields when compared to the Biot-Savart expression. Consequently, in this case, the simplified version of the wall can be considered a reasonable representation in the overall model to determine the effectiveness of the shielding. At Z = 1.0 metres, the maximum difference is 0.25 mT, which is considerably below the maximum difference of 3 mT in the source field.
Recommendation 7 for MICE Hall model: Simplified models of the shielding walls in the model should be adequate to determine if the flux density is low enough for equipment to be mounted behind them, unless the sensitive equipment is very close to discontinuities in the wall occurring because it is constructed from a finite number of plates. Substructure modelling will not be beneficial.

An assessment of the error in the source field associated with the finite element representation should be made in the same vicinity to determine whether the reduction of the field due to the shielding can be considered accurate.

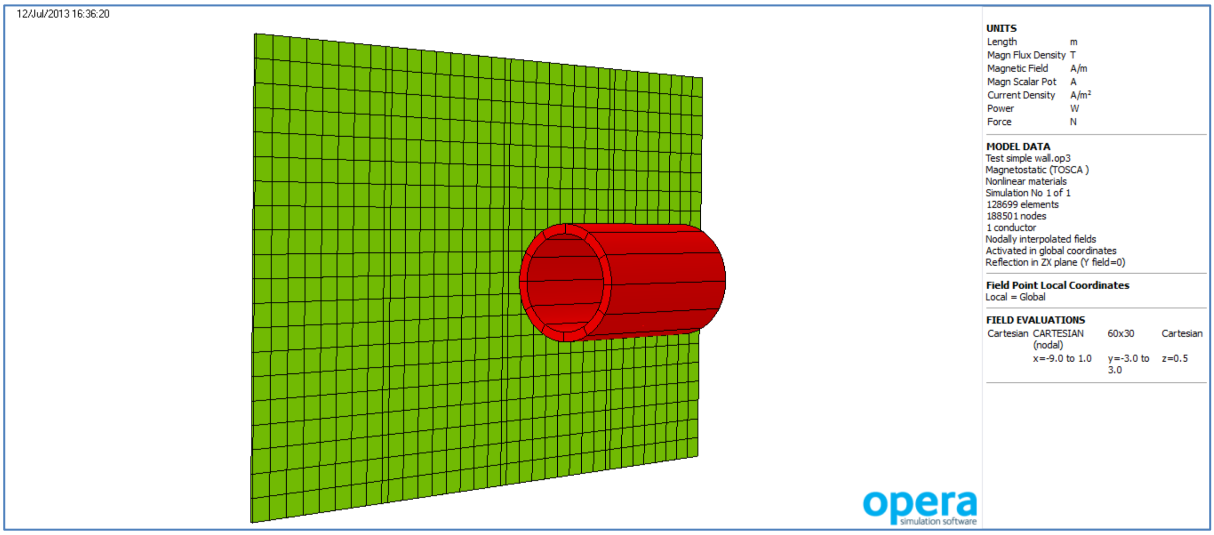

Figure 36: Geometry and mesh of simplified wall model

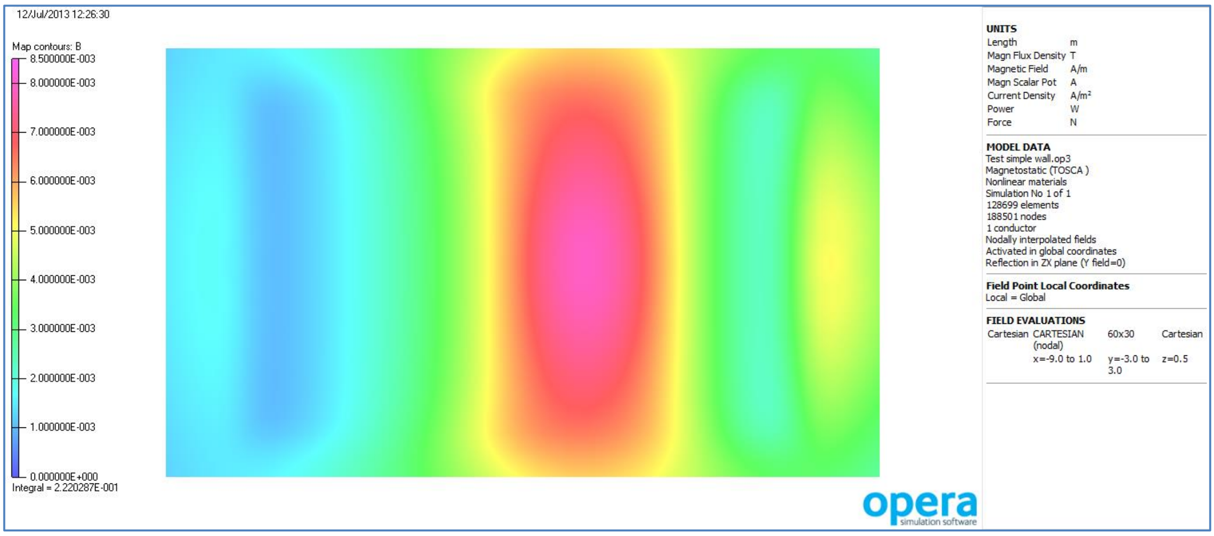

Figure 37: Flux density at Z = 0.5 metres for simplified wall model

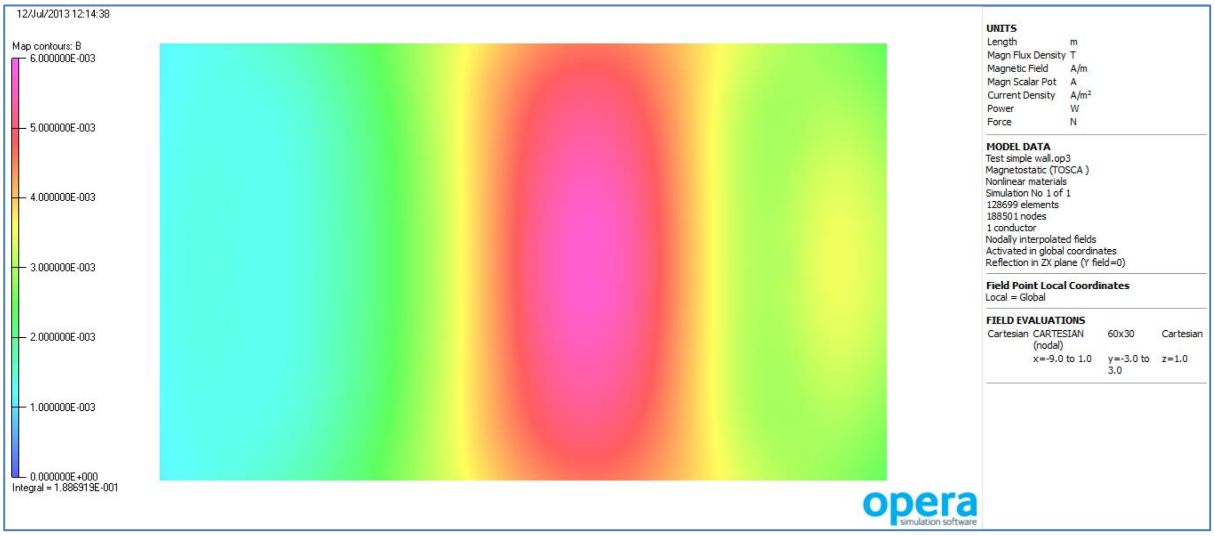

Figure 38: Flux density at Z = 1.0 metres for simplified wall model

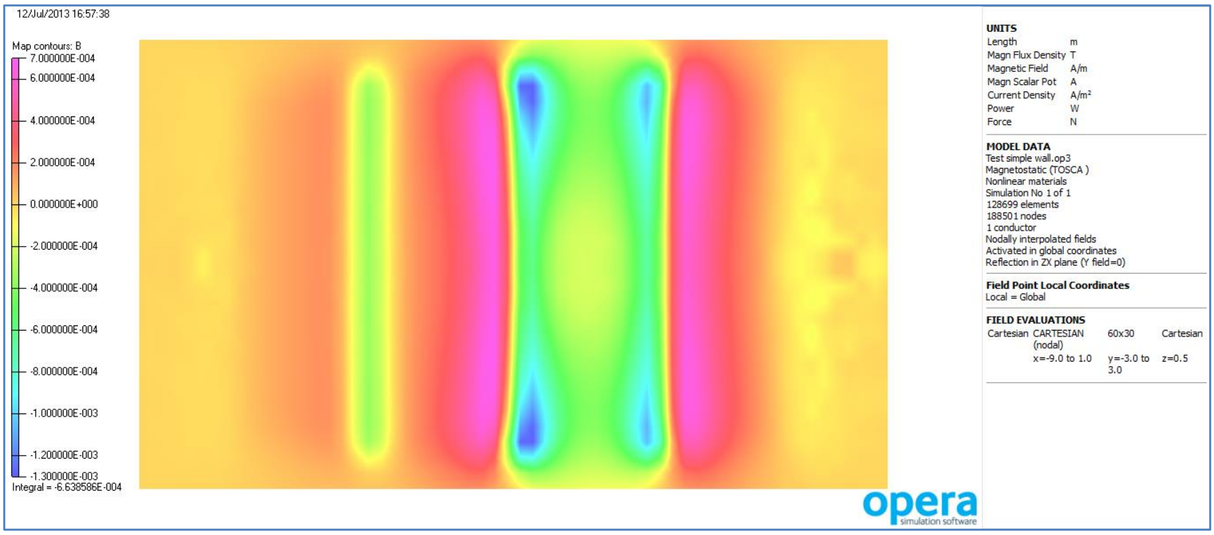

Figure 39: Difference in flux density at Z = 0.5 metres between simplified and "real" wall models

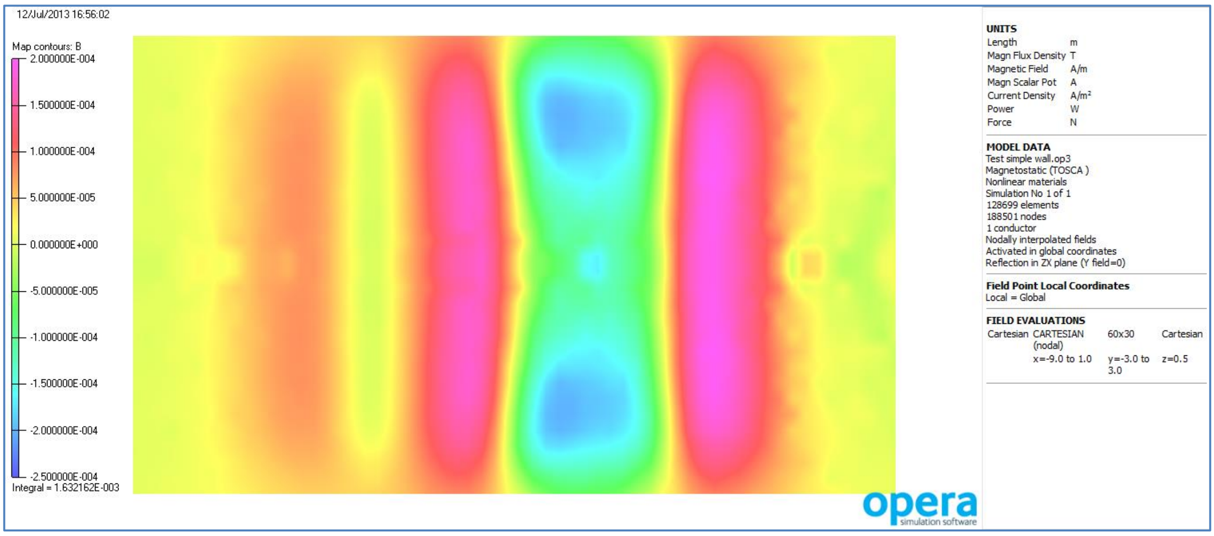

Figure 40: Difference in flux density at Z = 1.0 metres between simplified and "real" wall models

Conclusions

1. The effect of the meshing and truncation of infinite space should be assessed in any area where it is important to determine if sensitive equipment can be mounted. This should be achieved by comparing Biot-Savart calculated fields with fields recovered from the mesh assuming all materials have free-space permeability
2. Detailed substructure models can use the overall MICE Hall model to derive a source field providing:
    a. There is a simplified representation of the steel container and its contents included in the MICE Hall model
    b. The differences in the source field from the solenoids caused by using finite elements compared with Biot-Savart is not larger than the source field values for the sub-structure
3. Hollow tanks, or tanks with an equivalent centralized volume of magnetic material offer a better approximation than tanks completely filled with a dilute magnetic material
4. It is not accurate to extract the source field for a substructure model from a model of the MICE Hall that does not include a simple representation of the structure – see the earlier results obtained in the other MICE Hall report for including the "rack" in Model 91

5. Substructure modelling behind shielding walls should not be necessary unless the sensitive equipment is placed very close to discontinuities in the wall. The differences in source field associated with truncation of the mesh will probably be larger than the error introduced by simplification.